Discharge-rate persistence of baseline activity during fixation reflects maintenance of memory-period activity in the macaque posterior parietal cortex

Satoshi Nishida[1], Tomohiro Tanaka[1], Tomohiro Shibata[3],
Kazushi Ikeda[3], Toshihiko Aso[2], Tadashi Ogawa[1]

[1]Department of Integrative Brain Science, Graduate School of Medicine, Kyoto University, Sakyo-ku, Kyoto 606-8501, Japan
[2]Human Brain Research Center, Graduate School of Medicine, Kyoto University, Sakyo-ku, Kyoto 606-8501, Japan
[3]Mathematical Informatics Lab, Graduate School of Information Science, Nara Institute of Science and Technology, Ikoma, Nara 630-0192, Japan

Corresponding author: Tadashi Ogawa, PhD
Dept of Integrative Brain Science, Graduate School of Medicine, Kyoto University
Sakyo-ku, Kyoto 606-8501, Japan
Phone: +81-75-753-4678
FAX: +81-75-753-4486
e-mail: togawa@brain.med.kyoto-u.ac.jp

Brief running title: Baseline activity reflects delay-period activity

This is a pre-copyedited, author-produced PDF of an article accepted for publication in Cerebral Cortex following peer review. The definitive publisher-authenticated version is available online.

Abstract

Recent evidence has demonstrated that spatiotemporal patterns of spontaneous activity reflect the patterns of activity evoked by sensory stimuli. However, few studies have examined whether response profiles of task-evoked activity, which is not related to external sensory stimuli but rather to internal processes, are also reflected in those of spontaneous activity. To address this, we recorded activity of neurons in the lateral intraparietal area (LIP) when monkeys performed reaction-time and delayed-response visual-search tasks. We particularly focused on the target location-dependent modulation of delay-period activity (delay-period modulation) in the delayed-response task, and the discharge-rate persistency in fixation-period activity (baseline-activity maintenance) in the reaction-time task. Baseline-activity maintenance was assessed by the correlation between the spike counts of two separate bins. We found that baseline-activity maintenance, calculated from bins separated by a long interval (200–500 ms), was correlated with delay-period modulation, whereas that calculated from bins separated by a short interval (~100 ms) was correlated with trial-to-trial fluctuations in baseline activity, suggesting a link between the capability to hold task-related information in delay-period activity and the degree of baseline-activity maintenance in a timescale-dependent manner.

Keywords: spontaneous activity, delay-period activity, nonhuman primate, lateral intraparietal area, saccade

Introduction

Different neurons often respond in different ways even when they are located in the same cortical area and subjects are performing the same behavioral task. Although this cell-to-cell difference depends on a number of factors, such as sensory stimuli, cognitive processing, and motor preparation/generation, it may also be due to differences in the intrinsic response properties of individual neurons. Indeed, fluctuations in spontaneous activity reflect the intrinsic functional architecture of the brain in human imaging studies (for reviews, see Fox and Raichle 2007; Greicius 2008) and in animal electrophysiological studies (Arieli et al. 1996; Tsodyks et al. 1999; Kenet et al. 2003; Petersen et al. 2003; Fiser et al. 2004; Curto et al. 2009; Luczak et al. 2009; Ringach 2009; Sakata and Harris 2009). Thus, it is possible that cell-specific differences may produce different neuronal responses not only during task-evoked activity but also during spontaneous activity.

Previously, we particularly focused on the discharge-rate persistence in fixation-period activity (baseline-activity maintenance) in a visual search task. Because fixation-period activity is less influenced by voluntary eye movements and responses to visual stimuli compared with the activity during cognitive processes or behavioral actions, it may be suitable to infer the intrinsic response properties of a neuron. When comparing the degree of baseline-activity maintenance between two cortical areas, the frontal eye field (FEF) and area V4, we found that the ability to maintain the instantaneous discharge rate was greater for FEF neurons than for V4 neurons, suggesting a difference in the intrinsic storage capability across cortical areas (Ogawa and Komatsu 2010). However, that study did not answer the question of whether the degree of baseline-activity maintenance for a neuron actually correlates with the ability of that neuron to hold task-related signals in its activity during a task. More specifically, a neuron with a higher degree of baseline-activity maintenance could exhibit a greater ability to hold information about the target position in its delay-period activity in a memory-guided saccade task (Hikosaka and Wurtz 1983).

The lateral intraparietal area (LIP) is known to be a region in which robust and spatially

tuned activity is observed during the delay period in a memory-guided saccade task (e.g., Gnadt and Andersen 1988; Barash et al. 1991a, 1991b). Thus, the LIP is a suitable site to assess the above possibility. Here, we recorded neuronal activity from the LIP of monkeys performing reaction-time and delayed-response visual-search tasks, and examined the correlations between the degree of baseline-activity maintenance during fixation in the reaction-time task and the strength of target location-dependent modulation during delay in the delayed-response task (delay-period modulation). We found significant co-variability across neurons between the degree of baseline-activity maintenance and the strength of delay-period modulation. Our results suggest that the response properties observed in the baseline activity of a LIP neuron may be linked with intrinsic functional abilities that shape cell-specific responses in the task-evoked activity of that neuron.

Materials and Methods

Animal preparation and apparatus

Data were collected from two female macaque monkeys (*Macaca fuscata*, monkeys Y and S, 5.0 and 6.3 kg, respectively). A plastic head holder and recording chambers were secured to the skull using dental acrylic resin (Unifast II, GC, Aichi, Japan) and ceramic screws (Thomas Recording, Geissen, Germany) under deep anesthesia and sterile conditions. The recording chambers (inner diameter, 22 mm) were placed at stereotaxic coordinates (P2 and L21.5 for monkey Y; P4.1 and L18, and P0 and L21 for monkey S) above the intraparietal sulcus (IPS) with the assistance of magnetic resonance imaging (MRI) obtained before surgery (see below). An eye coil was surgically implanted beneath the conjunctiva of one eye (Judge et al. 1980). The monkeys were allowed to recover for 2 weeks prior to training and recording. All procedures for animal care and the experimental protocols were in accordance with the Guide for the Care and Use of Laboratory Animals of the National Research Council (1996) and were approved by the Animal Care and Use Committee of Kyoto University.

The experiments were under the control of two Windows XP-based computers that presented the stimuli, recorded neural signals and eye positions, and controlled the task schedule. They were developed using LabVIEW (National Instrument Japan, Tokyo, Japan) and C++ Builder (Borland Software Corporation, Scotts Valley, CA, USA). Visual stimuli were generated using a video-signal generator (ViSaGe; Cambridge Research Systems, Cambridge, UK) and presented on a video monitor with a 100-Hz refresh rate and 800 × 600 resolution (RDF223H; Mitsubishi, Tokyo, Japan). They were viewed binocularly from a distance of 42 cm in a dark room and subtended a visual angle of 51.5 × 40.0°. The luminance of stimuli and background was measured by a ColorCAL colorimeter (Cambridge Research Systems).

Single neurons were recorded using an epoxylite-insulated tungsten electrode (Frederick Haer & Co, Bowdoinham, ME, USA) with an impedance > 2 MΩ measured at 1 kHz (model IMP-1,

Bak Electronics, Germantown, MD, USA). Extracellular activity was amplified using a microelectrode AC amplifier (Model-1800; A-M Systems, Carlsborg, WA, USA) and stored on a computer equipped with a multichannel analog-to-digital board at a sampling rate of 50 kHz (PCI-6143, National Instrument Japan). Eye position was monitored and recorded using the scleral search coil technique (Fuchs and Robinson 1966) (eye position detector DSC-2001; Datel, Tokyo, Japan). Precise spikes were discriminated off-line using a template-matching method. Eye position signals were recorded at a sampling rate of 50 kHz but analyzed at 1 kHz resolution.

The recording site was determined using a guide-tube and a set of plastic grids that had holes spaced 1.0 mm apart and which were offset from each other by 0.5 mm. The guide tube (23 gauge) was lowered just above the dura matter surface, and the electrode penetrated the cortex through the dura using an oil hydraulic micromanipulator (MO-97A-S, Narishige, Tokyo, Japan). Under microscopic examination (OPMI-pico-i, Zeiss, Tokyo, Japan), a duratomy was made using fine forceps (Dumont No. 5) and a 25-gauge needle with the tip bent at a right angle. Only a small region of the tissue just below the selected grid hole was removed to avoid breaking the electrode. The chamber was filled with agarose (3%, A9793; Sigma, St. Louis, MO, USA) to promote recording stability. After each recording session, the dura matter surface was covered with anti-infective/anti-inflammatory ointment (Chlomy-P ointment, Daiichi-Sankyo, Tokyo, Japan).

Behavioral paradigms

Delayed-response visual-search task

This task was a variation of a memory-guided saccade task (Hikosaka and Wurtz 1983) (Fig. 1*A*). We analyzed neuronal activity of 94 LIP neurons obtained during this task. Each trial began with the appearance of a fixation spot at the center of a gray background (1 cd/m^2). The monkeys had to fixate on that spot within a window for typically 1000 ms, except for 13 cells (1,500–2,000 ms). The size of the window was ±1.2–1.6°, except for 17 cells (±2.5°). After sustained fixation, a cue stimulus was displayed at 8.5° eccentricity to indicate the

to-be-remembered target location (cue period, 500 or 700 ms). The target location was set with equal probability in the receptive field of the neuron under study or in the diametrically opposite location in the visual field. After fixation for a variable delay (800–1,800 ms), the fixation point was extinguished ("go" signal), and the monkeys were required to make a saccade toward the location at which the target had appeared during the cue period. If the monkeys made a single saccade landing inside a square window (±3.0 × 3.0°) centered on the target, another fixation point appeared at the target position. After 600 ms of fixation on this point, the monkey received a juice reward (successful trial). An inter-trial interval (300–2,000 ms) was imposed before the beginning of a next trial after a trial ended. If the monkey made a saccade toward the location outside the target-centered window or could not keep the fixation within the window for 600 ms, the trial was immediately terminated with no reward (erroneous trial).

A cue stimulus was either an isolated stimulus (isolated-stimulus trial) or an array stimulus (array-stimulus trial). In the isolated-stimulus trials, a circle (10 cd/m^2; 2.24° in diameter) was presented as a target. Its color was either white (CIE chromaticity coordinate: x = 0.29, y = 0.32), orange (x = 0.43, y = 0.47 for monkey Y; x = 0.44, y = 0.46 for monkey S), yellowish-orange (x = 0.41, y = 0.48 for monkey Y; x = 0.42–0.43, y = 0.47 for monkey S), green (x = 0.24, y = 0.41 for monkey Y; x = 0.23, y = 0.37–0.39 for monkey S), or bluish-green (x = 0.23, y = 0.38 for monkey Y; x = 0.22, y = 0.34 for monkey S). In the array-stimulus trials, one singleton element (target), unique in color, and five additional identical elements (distractors) were simultaneously presented. All elements were isoluminant circles (10 cd/m^2; 2.24° in diameter) with the same colors as used in the isolated-stimulus trials. Target and distractor colors were set to either orange/green, green/orange, yellowish-orange/bluish-green, or bluish-green/yellowish-orange. Each color pair was presented at the equal probability. Of the 94 cells studied, data from 73 were recorded during both the isolated and array-stimulus trials, and data from the remaining 21 were recorded only during the isolated-stimulus trials.

Reaction-time visual search task

The procedure for this task was the same as that in the delayed-response visual-search task, except that no delay period was imposed (Fig. 1*B*), the number of color pairs for array stimuli was increased, and target-absent trials were introduced. After fixation, either an isolated or an array stimulus was displayed, and the monkeys were required to make a saccade toward the target without an artificial delay. When the computer detected a saccadic eye movement, the visual stimuli and the fixation spot were immediately extinguished. In the isolated-stimulus trials, an orange, yellowish-orange, green or bluish-green circle (10 cd/m^2) was presented as a target. In the array-stimulus trials, one color-singleton target was presented with five identical distractors. All six elements were isoluminant (10 or 1 cd/m^2). Target- and distractor-color pairs were selected so that their color similarity was either small (orange/green, green/orange, yellowish-orange/bluish-green, or bluish-green/yellowish-orange) or large (yellowish-orange/orange, orange/yellowish-orange, bluish-green/green, or green/bluish-green). The stimulus colors in both trials were the same as those used in the delayed-response task. In addition to these target-present trials, target-absent trials were also interleaved. If all six elements had one of the four colors, the monkeys had to maintain their fixation (800–1800 ms) until the end of the trial (target-absent trials).

Trials of delayed-response (17–23%) and reaction-time (77–83%) visual search tasks were implemented pseudo-randomly. The eccentricity of the visual stimuli were fixed at 8.5° in the periphery to minimize inter-neuron differences in task difficulty across recording sessions, because behavioral performance during visual search varies with retinotopical eccentricity (e.g., Carrasco and Yeshurun 1998; Wolfe et al. 1998; Meinecke and Donk 2002). The task type was instructed by the color or shape of the fixation spot. A white circle (0.39–0.55° in diameter) was presented during the reaction-time task, whereas either a yellow circle or white square (0.39–0.55° in diameter) was presented during the delayed-response task. For a minority of cells (13/94 = 14%), trials of both tasks were conducted separately.

Data collection

Single-cell activity was recorded by advancing electrode into the lateral bank of the IPS. Once a neuron was isolated, we initially assessed the location of the receptive field using the delayed-response task. An isolated stimulus was presented at one of six evenly separated directions on an imaginary circle (eccentricity = 8.5°), because the stimulus-location eccentricity was fixed at 8.5° during the visual search tasks. We manually adjusted those six directions so that one direction evoked the strongest activity.

Before starting the present experiment, we specified the IPS location based on the response properties; the medial bank of the IPS tended to exhibit activity related to somatosensory stimuli, whereas the lateral bank exhibits visual and saccade-related responses (Mountcastle et al. 1975; Barash et al. 1991b; Maimon and Assad 2006). After specifying the IPS locus, we started to record neurons in the lateral bank of the IPS from a region regarded as the LIP in which neurons exhibit robust, spatially tuned responses during the delay period of a memory-guided saccade task (Gnadt and Andersen 1988; Barash et al. 1991a, 1991b; Colby et al. 1996; Shadlen and Newsome, 2001). To ensure that our samples were in area LIP rather than area 7a, neurons recorded at a depth shallower than 3 mm from the dura surface were excluded from the present analysis (Andersen et al. 1990; Linden et al. 1999; Gifford and Cohen 2004). Neurons were typically recorded at > 5 mm depth from the dura surface (85%), and the majority of our neurons (56%, see Results) exhibited significant modulations in delay-period activity (determined by whether activity 100–700 ms before the go signal differed significantly according to target location; Mann–Whitney *U*-test, $P < 0.05$). This fraction was comparable to that reported for the LIP in previous studies (e.g., Barash et al. 1991a; Maimon and Assad 2006; Falkner et al. 2010).

To verify the recording positions, we acquired post-operative structural MRIs for both monkeys on a 0.2 Tesla open whole-body scanner (Signa Profile; General Electric, Milwaukee, WI, USA). The advantage of this low-magnetic field system is the reduced distortion of the original

cortical structures (Petersch et al., 2004). We used a three-dimensional spoiled, gradient-recalled pulse sequence with the following parameters: TR = 29 ms, TE = 8.3 ms, flip angle = 40°, field of view = 16 cm, 256 × 256 matrix, 100 slices, voxel size = 0.63 × 0.63 × 1.0 mm. To improve image signal-to-noise ratio, we aligned and averaged two or three acquisitions during post-processing. Figure 2 shows images from one monkey (monkey Y). We used five plastic tubes filled with an 84–87% glycerin solution (Glycerin P, Kenei, Tokyo, Japan) to be visible in the MRI to determine the plane and trajectory of the electrode penetrations (Fig. 2*A*). These tubes were embedded in a plastic base attached to the recording chamber so that one was the center and the remaining four were arranged in the x-y coordinate (8 mm apart from the center) of the recording grid (Fig. 2*B*). The penetration sites on the brain surface were reconstructed based on the coordinates determined by the positions of the reference tubes and recording grids. The number of cells recorded from each grid location is illustrated in Figure 2*C*. Figure 2*D* shows the MRIs that matched the plane of the recording penetrations. The zone of the recording sites (arrow heads), which was reconstructed from a combination of grid sites and recording depth, is superimposed on the MRIs. Figure 2*E* shows coronal MRIs representing the most anterior to the most posterior recording positions. We similarly verified recording positions for another monkey (monkeys S) by acquiring post-operative MRIs. Thus, our samples were presumably recorded from the LIP based on the physiological properties of the recorded neurons and verification by the MRIs.

Data analysis

We constructed interspike interval (ISI) distribution histograms to confirm adequate spike isolation. Neurons were included in the analysis if they maintained stable spike isolation throughout the recording session and if their distribution histograms showed no ISIs < 2 ms (the refractory period). Unless otherwise indicated, only data from successful trials were analyzed. Spike density functions were constructed with 1 kHz resolution by convolving spike trains with a Gaussian function (SD = 10 ms) (Richmond et al. 1987). Population average spike density functions were constructed by averaging the spike density functions from individual neurons.

Analysis of saccadic eye movements

Horizontal and vertical eye velocity signals were calculated by digitally differentiating horizontal and vertical eye position signals, respectively. Saccades were detected using a computer algorithm that identified the initiation and termination of each saccade based on a velocity-threshold criterion. Change in eye velocity was recognized as a saccade if it was greater than the threshold of 120°/s for at least 10 ms. The initiation of a saccade was defined as the time at which the velocity increased to >30°/s.

Analysis of discharge-rate maintenance in baseline activity

To assess the persistence of the instantaneous discharge rate in baseline activity, we focused on pre-stimulus activity during fixation (the activity in an 800-ms interval prior to stimulus onset). Because the monkeys were required to maintain their gaze directed toward the central spot on the display during the fixation period and had no information about the forthcoming visual stimuli, baseline activity was virtually free of any voluntary eye movements and response to task-related visual stimuli except the fixation spot. This allowed us to examine response properties of individual neurons under conditions in which the effects of visual sensory stimuli and eye movements may be at a minimum. We examined the pre-stimulus baseline activity obtained from both the reaction-time and delayed-response tasks. In particular, we were more interested in the baseline activity in the reaction-time task, because it was possible that baseline activity in the delayed-response task could be modulated by the readiness to the task requiring the monkeys to remember the spatial location of a target. Indeed, previous studies have demonstrated that pre-stimulus baseline activity in the LIP is modulated by the demands of the task at hand (Toth and Assad 2002; Stoet and Snyder 2004). Taken together, by examining the fixation-period activity in the reaction-time task, we could access an automatic process for activity maintenance rather than an active process driven by task demands. To ensure sufficient spike data for analysis, we examined only neurons in which the number of trials was > 100 and the mean activity during the 800-ms interval before array presentation was > 5

spikes/s. Of 119 neurons we recorded, 94 neurons fulfilled these criteria. The results were essentially the same when the spike-rate threshold varied between 1 and 10 spikes/s.

To intuitively illustrate baseline-activity maintenance, we separated the trials into three groups (high, medium, and low activity) according to the spike counts during the 100-ms interval 400–500 ms before array presentation. The distribution of spike counts during each trial was fitted to a Poisson distribution. The thresholds for trial classification were determined based on the one-third and two-thirds levels of the cumulative probability of the distribution. Then we calculated the spike-density function for each of the trial groups. We expected that the difference in spike-density functions at a given time would persist for a long period if a neuron stored its instantaneous discharge rate for the long term; if not, the differences in spike density would diminish after a short interval.

To quantitatively characterize baseline-activity maintenance, we calculated the temporal correlations between spike counts per bin within a trial (temporal correlation analysis), as described in Ogawa and Komatsu (2010). We first divided the 800-ms fixation period prior to stimulus onset into eight successive 100-ms time bins and counted spikes in each bin of individual trials. The mean spike count across trials in a given bin was subtracted in advance from the spike counts of individual trials in that bin. Next, we produced spike-count pairs of bins separated by intervals of 100, 200, 300, 400, 500, 600, or 700 ms. Then we calculated the Pearson's correlation coefficient using all pairs of bins with each separation interval. For example, to calculate the temporal correlation with a 300-ms separation from a dataset of 100 trials, the spike count data from five pairs of bins (1st-4th, 2nd-5th, 3rd-6th, 4th-7th, and 5th-8th bins) for each trial were pooled across all trials (500 spike-count pairs = 5 pairs/trial × 100 trials), and then one correlation coefficient value was computed using these 500 spike-count pairs. The coefficients were used as the index of baseline-activity maintenance, termed the within-trial baseline discharge-rate maintenance (within-trial BM) index. We also calculated an across-trial BM index (i.e., shift predictor) to estimate the strength of the correlations resulting from

inter-trial changes in baseline activity, which indicates the correlation between spike counts in one bin during a given trial and that in the other bin during the following trial. As described above, because the mean spike count across trials in each bin was subtracted from the spike counts of individual trials in that bin, the within-trial BM index reflected the correlation between the spike-count deviations from the mean spike count in one bin and those in another bin. Consequently, if a neuron has the high ability to hold its discharge rate, the stronger discharge rate would persist for a while when the discharge rate is stronger than its mean value in a given bin, whereas the weaker discharge rate would persist if the discharge rate is weaker than its mean value in a given bin. Therefore, this index can robustly measure the degree of the discharge-rate persistency, even if the mean discharge rate is not constant but rather has an unstable temporal pattern during fixation.

If the discharge rate of baseline activity slowly drifted across trials, this slow drift could generate quasi-significant correlations in the temporal correlation analysis even in the absence of actual correlations between the spike counts of the separate bins within a trial. To avoid this effect on the temporal correlation analysis, we only analyzed the baseline activity of those trials in which the mean discharge rates of the fixation-period activity were not statistically different across trials. To this end, we chose 100 successive trials (a 100-trial window) during a recording session, divided them into four successive 25-trial groups, and determined significant differences in the strength of activities across the four groups using the Kruskal–Wallis test. By moving a 100-trial window in one-trial steps from the first to the last trial in each recording session, we determined the longest successive set of trials in which activity strength did not differ significantly (Kruskal–Wallis test, $P > 0.01$). Applying this statistical pretreatment, 138–818 trials (mean ± SD = 365 ± 160 trials; 27.7–100% of all trials, mean ± SD = 67.9 ± 22.9%) were chosen and used for the current analyses. As we will show, this manipulation was not essential for obtaining our main findings.

Analysis of delay-period modulations of task-evoked activity

In the delayed-response task, animals had to remember the spatial location of a previously

presented target to make a saccade to that location after the delay. Many studies have demonstrated that LIP neurons exhibit spatially tuned responses during the delay period (e.g., Gnadt and Andersen 1988; Barash et al. 1991a, 1991b; Colby et al. 1996; Shadlen and Newsome 2001; Bisley and Goldberg 2003, 2006). Delay-period activity is thought to be related to the activity that is evoked by internal (endogenous) factors, such as memory, spatial attention, and/or motor preparation, rather than the activity that is directly driven by sensory (exogenous) factors. In this context, we consider delay-period activity as "task-evoked" activity. To quantitatively evaluate the strength of target direction-dependent modulation in the task-evoked activity for each neuron, we computed a delay-period modulation (DM) index defined as $|R_{in} - R_{away}|/(R_{in} + R_{away})$, where R_{in} and R_{away} refer to the mean discharge rate during trials in which the target appeared inside the receptive field and those in which the target appeared outside the receptive field, respectively. A value close to 1 indicated that the difference in discharge rate between the two stimulus conditions was substantial (i.e., strong delay-period modulation), whereas a value close to 0 indicated little difference between the two stimulus conditions (i.e., weak delay-period modulation). To reduce the possibility that the DM index was substantially influenced by a decay in visually evoked activity or saccade eye movement-related activity, the activity was measured as the spike count per trial during a 600-ms interval from 100 to 700 ms before the disappearance of the fixation spot: starting at a mean of 544 (±217 *SD*) ms after target disappearance and ending at a mean of 283 (±43 *SD*) ms before saccade onset.

Analysis of trial-to-trial fluctuations in baseline activity

We calculated Fano factors by dividing the variance in the spike count by its mean to assess trial-to-trial fluctuations in baseline activity. We measured the Fano factors for each neuron from the spike counts in baseline activity during each consecutive 100-ms bin during the 800 ms before search-array presentation and averaged them across bins.

Analysis of response types of neurons

Manifestations of visually responsive and saccade-burst activity were examined using data sets from the isolated-stimulus trials during the delayed-response visual-search task. A neuron was defined as exhibiting visually responsive activity when the activity occurring from 50 to 150 ms after array presentation was significantly greater than the pre-stimulus activity occurring from 200 to 400 ms before the array presentation (Mann–Whitney *U*-test, $P < 0.05$). A neuron was defined as exhibiting saccade-burst activity if its activity during a 100-ms interval prior to saccade initiation was significantly greater than its preceding delay-period activity during a 100-ms interval starting 300 ms before the initiation of a saccade (Mann–Whitney *U*-test, $P < 0.05$) (Lawrence et al. 2005). Then we classified neurons into three types: neurons with only visually responsive activity (visual neurons), those with only saccade-burst activity (movement neurons), and those with both responses (visuomovement neurons).

Results

Neuronal database

Recordings were made from three hemispheres of two macaques (one hemisphere in monkey Y and both hemispheres in monkey S). Only neurons that maintained stable spike isolation throughout the recording session and showed ISI distribution histograms with no ISIs < 2 ms were included in the analysis. In total, 119 neurons were classified as being in the LIP based on the anatomical and physiological criteria (see Materials and Methods). Of them, 94 neurons (31 from monkey S and 63 from monkey Y) fulfilled the criteria for appreciable baseline activity during the 800 ms before stimulus onset in the reaction-time task (≥5 spikes/s, 5.0–56.6 spikes/s, mean ± SD = 17.3 ± 11.3 spikes/s) and for sufficient trials in both the reaction-time task (≥100 trials, 138–818 trials, mean ± SD = 365 ± 160 trials) and the delayed-response task (≥4 trials under each stimulus condition, 4–99 trials, 23 ± 15 trials). We used these 94 neurons for data analysis in this study.

Baseline-activity maintenance and delay-period modulation of single LIP neurons

Figure 3*A*–*D* shows the response profiles from one LIP neuron. Figure 3*A* shows neuronal activity during the reaction-time visual-search task from 693 successful trials. To intuitively show the ability of baseline-activity maintenance, we separated trials into three groups according to the activity strength in a brief interval and compared these groups. Figure 3*B* shows three spike-density functions of the high- (red), medium- (green), and low-activity (blue) groups classified based on the 100-ms interval 400–500 ms before array presentation (gray rectangle in Fig. 3*B*). A significant activity difference between the high- and low-activity groups persisted not only during the 100 ms used for trial separation but also during the remaining fixation period (horizontal black line; Mann–Whitney *U*-test, $P < 0.01$), indicating strong maintenance of the instantaneous discharge rate during baseline activity. Similar results were observed when the trials were grouped according to the activity strength of the other 100-ms bins during the fixation period. To quantitatively evaluate the ability of baseline-activity maintenance, we computed the baseline discharge-rate maintenance indices (BM indices) that reflected the strength of the correlation between the spike counts in two

100-ms bins. Figure 3*C* shows the values of the within-trial (circles) and across-trial (squares) BM indices as a function of the time separating two bins. Although the strength of the within-trial BM indices gradually decreased as separation time increased, it was significantly greater than zero at all separation times except 600 and 700 ms (black circles; Pearson's correlation, $P < 0.01$), indicating that this cell possessed the ability to retain its instantaneous discharge rate up to 500 ms. In contrast, the across-trial BM indices were close to zero (-0.01–0.017) and not significantly different from zero at all separation times (white squares; Pearson's correlation, $P > 0.4$), indicating that the maintenance of baseline activity was not the result of neural modulation across trials but rather of neural modulation within a trial.

Then we examined the strength of delay-period modulations in the delay-response visual-search task. Figure 3*D* shows the activity when an isolated target appeared inside the receptive field (black trace) and when it appeared outside the receptive field (gray trace). We found a profound difference in delay-period responses depending on the location of the target (Mann–Whitney *U*-test, $P < 0.0001$). To quantify the ability of this neuron to signal the target location during the delay, we calculated a delay-period modulation (DM) index that reflected the difference in activity between trials when the target appeared inside and outside the receptive field. The DM index of this neuron was 0.83.

Figure 3*E–H* shows the response profile of another LIP neuron. The degree of baseline-activity maintenance was considerably weaker in this neuron (Fig. 3*F*). When trials (454 successful trials) were separated into three groups according to the strength of instantaneous activity, the significant difference between the high- and low-activity groups was restricted to the period in and around the 100-ms interval used for trial separation (horizontal black line; Mann–Whitney *U*-test, $P < 0.01$). The temporal correlation analysis of baseline activity consistently revealed that the values of the within-trial BM indices were not different from zero (Fig. 3*G*; Pearson's correlation, $P > 0.02$) except for a 200-ms separation time (Pearson's correlation, $P < 0.01$). Moreover, although

delay-period modulation was significant (Fig. 3*H*, Mann–Whitney *U*-test, $P = 0.024$), its magnitude was very small (DM index = 0.12).

Thus, one neuron with strong baseline-activity maintenance exhibited substantial delay-period modulation, whereas another neuron with weak baseline-activity maintenance exhibited poor delay-period modulation. These results suggest that the neuron-to-neuron variability in baseline-activity maintenance during fixation is potentially associated with that in delay-period modulation of task-evoked activity. In the following analyses, we sought to assess this potential link at the population level.

Population analyses of baseline-activity maintenance

To determine the degree of baseline activity maintenance at the population level, we calculated the BM indices for each of 94 LIP neurons using the baseline activity in the reaction-time task. Figure 4*A* shows the values of the within-trial BM index as a function of separation time. The mean within-trial BM indices (thick black line) decreased gradually as separation time increased (Spearman's correlation, $\rho = -0.57$, $P < 0.0001$). At the level of individual neurons, the degree of baseline-activity maintenance varied largely from neuron to neuron (thin gray lines). The values of the within-trial BM indices were significantly greater than zero in 95%, 95%, 83%, 76%, 50%, 38%, and 26% of the neurons at separation times of 100, 200, 300, 400, 500, 600, and 700 ms, respectively (Pearson's correlation, $P < 0.01$). We found no neuron in which the within-trial BM index was significantly less than zero (Pearson's correlation, $P > 0.01$). This result indicates that almost all neurons (>90%) maintained the discharge rate for a period ranging from 100 to 200 ms, whereas about one-third or one-fourth of neurons (<40%) did so for up to 600 or 700 ms. Figure 4*B* shows the across-trial BM indices. In contrast to that of the within-trial BM index, the strength of the across-trial BM index was rather low across neurons. In only a minority of neurons, the across-trial BM index was significantly different from zero (Pearson's correlation, $P < 0.01$): 17%, 15%, 12%, 6%, 9%, 5%, and 3% of neurons at separation times of 100, 200, 300, 400, 500, 600, and 700 ms,

respectively. Overall, the mean across-trial BM indices were significantly lower than the mean within-trial BM indices at all separation times (paired *t*-test, $P < 0.0001$).

To confirm that these observations were not limited to the BM indices obtained using a particular bin size (100 ms), we calculated the BM indices using the other bin widths (50, 200, and 300 ms). The mean within-trial BM indices decreased gradually as a function of increases in separation time (Supplementary Fig. 1*A*; Spearman's correlation, ρ = -0.57, -0.50, and -0.39 for bin widths of 50, 200, and 300 ms, respectively, $P < 0.0001$), and the mean across-trial BM indices were close to zero irrespective of separation time (0.008–0.037; Supplementary Fig. 1*B*), consistent with the results observed when a 100-ms bin width was used for the calculation. Therefore, the following analyses were conducted using the BM indices calculated with a 100-ms bin width unless otherwise indicated.

Before starting the fixation in each trial, the eye position was not restricted. Therefore, there is the possibility that that differential visually-evoked and/or saccade-related activity might be elicited when the monkeys made saccades to the fixation spot from different locations. If such differential activity lasted, this could yield false temporal correlations in baseline activity. In this case, it is expected that the BM indices were reduced as the fixation time increased, because visual and saccadic responses should gradually diminish after the onset of fixation. To test this possibility, we examined how the within-trial BM index changed depending on the time during the fixation period. The result shows that the magnitude of the BM indices tended to hold during fixation (Supplementary Fig. 2*A*), indicating that it is unlikely that visual responses and prefixation eye movements were responsible for producing the temporal correlations observed in baseline activity.

In our recordings, the fixation duration prior to stimulus presentation was typically fixed (1,000 ms), but it was variable (1,500–2,000 ms) for a minority of cells. This difference in the fixation period did not produce any difference in the degree of baseline-activity maintenance. We

compared the within-trial BM indices between two groups of neurons separated according to whether the fixation duration was fixed (n = 81) or variable (n = 13), and found no difference between them at all separation times (Supplementary Fig. 2*B*; two-sample t-test, $P > 0.07$).

Previous studies have shown that the correlation between spike trains increases with firing rate (De la Rocha et al., 2007). To test whether the observed correlations were due to higher discharge rates of baseline activity, we examined the dependence of the BM indices on the discharge rate of baseline activity. Although the discharge rate during the 800-ms interval preceding the array presentation varied from neuron to neuron (5–57 spikes/s, mean ± SD = 17 ± 11 spikes/s), we found no significant correlation between the discharge rate and the BM indices at all separation times across neurons (Pearson's correlation, r = -0.06–0.17, $P > 0.09$), indicating that the BM index did not depend on the discharge rate in baseline activity.

Population analyses of delay-period-activity modulation

We calculated the DM index for each of the 94 LIP neurons. Figure 5*A* shows the distribution of the DM indices, which varied across neurons (0–0.83, mean ± SD = 0.25 ± 0.22). Significant delay-period modulation was observed in 56% (53/94) of the neurons studied (gray bar in Fig. 5*A*; Mann–Whitney U-test, $P < 0.05$). To illustrate the relationship between the DM index and the time course of activity during the delayed-response task, the 94 neurons were divided into three groups based on the two threshold levels corresponding to one-third and two-thirds of the difference between the minimum and maximum DM indices, and the average spike-density functions were calculated separately for each group (Fig. 5*B*–*D*). Delay-period modulation was prominent for neurons with high DM indices (Fig. 5*B*), moderate for neurons with medium DM indices (Fig. 5*C*), and weak for neurons with low DM indices (Fig. 5*D*), assuming that the currently defined DM index is an appropriate measurement of the strength of the task-related modulation in delay-period activity.

For further confirmation to exclude the influence of decaying visually evoked activity on

the DM indices, we calculated these indices using the delay-period activity from the array-stimulus trials (Supplementary Fig. 3*A*). Because isoluminant target or distractor elements were always presented in the receptive field of the neuron during the cue period of the array-stimulus trials, the difference between visual responses when the target appeared inside the receptive field and that when it appeared outside the receptive filed should have been substantially reduced compared to that during the isolated-stimulus trials. The cell-to-cell variation in the DM indices for the array-stimulus trials was consistent with that in the isolated-stimulus trials (Supplementary Fig. 3*B*), indicating that delay-period modulations were unlikely to be explained by the effects of decaying stimulus-driven activity evoked by a cue stimulus.

Effects of trial-to-trial fluctuations in baseline activity

To know the relationship between the degree of baseline-activity maintenance (within-trial BM index) and the strength of delay-period modulation (DM index), we calculated the raw correlation between the two indices across our sample of 94 neurons (Fig. 6). Figure 6*A* shows the relationship between the DM indices and the within-trial BM indices, which were calculated from bins separated by either 100-, 300-, or 500-ms intervals. Interestingly, the correlation coefficients were significant for the BM indices with a 300- or 500-ms separation (Pearson's correlation, $r = 0.44$ and 0.22, respectively, $P < 0.05$), but not a 100-ms separation (Pearson's correlation, $r = 0.18$, $P = 0.08$). Figure 6*C* summarizes the dependence of the correlation between the DM and the within-trial BM indices on separation time (see also Supplementary Table 1). The strength of the correlation was strongest at a separation time of 300 ms and decreased gradually as separation time increased or decreased from that separation time (black bars in Fig. 6*C*).

This result seems implausible because the average within-trial BM index was strongest at 100 ms of separation and monotonically decreased as separation time increased (Fig. 4*A*). What mechanisms explain this discrepancy? It is generally known that the discharge rate in baseline activity fluctuates from trial to trial. Such trial-to-trial fluctuations evaluated with Fano factors in

baseline activity could affect the strength of the within-trial BM index. Indeed, we found a significant raw correlation between the Fano factor (variance/mean spike count in a 100-ms window) and the within-trial BM index at 100 ms of separation (Fig. 6*B*; Pearson's correlation, $r = 0.47$, $P < 0.0001$), suggesting that the influence of trial-to-trial fluctuations may interfere with the correlation between the DM and the within-trial BM indices at short separation times (~100 ms).

Analysis of partial correlations between baseline-activity maintenance, delay-period modulation, and Fano factors

To determine whether the variables were actually correlated, we calculated the partial correlation between the DM and the within-trial BM indices, factoring out their association with the Fano factor, and similarly calculated the partial correlation between the within-trial BM index and the Fano factor, factoring out the DM index. The Fano factor was significantly correlated with the within-trial BM index, particularly at a separation time of 100 ms (gray bars in Fig. 6*D*, Pearson's partial correlation, $r = 0.47$, $P < 0.05$), whereas the DM index was significantly correlated with the within-trial BM index at separation times ranging from 200 to 500 ms (black bars in Fig. 6*D*, Pearson's partial correlation, $r = 0.22$–0.44, $P < 0.05$) (all r and P values are summarized in Supplementary Table 1). We found no significant correlation between the DM index and the Fano factor (Pearson's correlation, $r = 0.035$, $P = 0.73$). These results suggest that the strength of delay-period modulation may be linked with the degree of longer-term maintenance (200–500 ms) of baseline activity, whereas the trial-to-trial fluctuations may be linked with the degree of short-term maintenance (~100 ms).

To confirm the robust association between the baseline-activity maintenance and the delay-period modulation, we performed the same partial correlation analysis when the delay-period modulation was measured in two different ways. When a partial correlation was calculated using the DM indices obtained from the array-stimulus trials instead of the isolated-stimulus trials (Supplementary Fig. 3*C*), or when it was calculated using an alternative measurement for

delay-period modulation (the delay-period discharge rate when the target appeared inside the receptive field vs. the baseline discharge rate, Supplementary Fig. 4), the results were essentially the same.

In this study, to avoid the possibility that slow drifting activity could generate the quasi-significant BM indices, we only analyzed the baseline activity of those trials in which the mean discharge rate of baseline activity was stable across trials (see Material and Methods). Such a data preprocessing step was not crucial to obtain the present data. Even when we performed the data analysis without this preprocessing, the results were essentially the same (Supplementary Fig 5).

Our description of the results thus far has relied on a particular bin width (100 ms) and a particular set of separation times (ranging from 100 to 700 ms, with a resolution of 100 ms) for computing the BM index. These values were not crucial for obtaining the present results. To demonstrate this, we conducted partial correlation analysis using various combinations of separation times (range: 10–790 ms, 10-ms resolution) and bin widths (range: 40–400 ms, 10-ms resolution). Figure 7*A*, *B* shows the Pearson's partial correlation coefficients between the DM and within-trial BM indices and those between the within-trial BM indices and the Fano factors. The correlation coefficient between the DM and within-trial BM indices increased when separation time ranged from 200 to 400 ms (the strongest coefficient, 0.46, was obtained at a 310-ms separation time and a 100-ms bin width), whereas that between the within-trial BM indices and the Fano factors was strongest at separation times of 100 ms or less (the strongest coefficient, 0.75, was obtained at a 40-ms separation time and a 40-ms bin width), confirming the findings presented in Figure 6*D*. In addition, when the Fano factor was computed using a bin width other than 100 ms (25–800 ms), virtually the same results were obtained.

Control analyses

Our results showed a significant correlation between baseline-activity maintenance during

fixation and delay-period modulation (Fig. 6*D*). However, it is possible that other factors commonly affected both baseline-activity maintenance and delay-period modulation and produced a spurious correlation between them. To assess this issue, we performed a series of control analyses to test whether other factors could explain the present results.

We have thus far focused on the degree of baseline-activity maintenance obtained from trials in the reaction-time visual search task. Therefore, we tested whether the present results were still preserved when the BM index was evaluated based on the baseline-activity in the delayed-response task rather than the reaction-time task. Although the differences in the mean values of the within-trial BM indices were significant at all separation times except for 200 ms (paired *t*-test, $P < 0.05$), their differences were small and exhibited very similar dependencies on separation time between the delayed-response and the reaction-time tasks (Supplementary Fig. 6*A*). Then we performed the same partial correlation analysis for the within-trial BM indices derived from the delayed-response task (Supplementary Fig. 6*B*). The DM index was significantly correlated with the within-trial BM index with longer separation times ranging from 400 to 500 ms, whereas the Fano factor was significantly correlated with the within-trial BM index with a separation time of 100 ms (Pearson's partial correlation, $P < 0.05$). Although we found that the separation time at which the correlation with the DM index was the strongest was longer in the delayed-response task (500 ms, Supplementary Fig. 6*B*) than that in the reaction-time task (300 ms, Fig. 6*D*), there is the possibility that this difference may be caused by the small number of cells and trials in the delayed-response task (55 cells and 163 trials on average) compared with those in the reaction-time task (93 cells and 365 trials on average). But, when the number of cells and trials were matched between the tasks, the distribution of correlation coefficients in the reaction time task did not change substantially (compare Fig. 6*D* with Supplementary Fig. 6*C*), suggesting that the difference between tasks was not caused by the size of the data set. Nonetheless, the present results that the within-trial BM indices with longer and shorter separation times were separately correlated with the DM index and the Fano factor, respectively, were preserved even when the BM index was calculated from the baseline

activity in the delayed-response task rather than the reaction-time task.

Next, we assessed the influences of motivation/behavioral performance. Previous studies have reported that neuronal activity during the fixation period varies predictably according to the expected trial state (success/error) and impending saccadic reaction time, reflecting the motivational level of a monkey (Kobayashi et al. 2002; Okada et al. 2009). Consequently, one may argue that the association between stronger baseline-activity maintenance (within-trial BM index) and stronger delay-period modulation (DM index) in a given recording session simply reflects session-to-session differences in motivational level. To assess this possibility, we examined the associations of the DM and within-trial BM indices with performance scores and saccadic reaction times. Because the average performance score and the mean saccadic reaction time across sessions differed significantly between the two monkeys (performance score: 73.5 ± 5.3% vs. 80.3 ± 6.1%, two-sample *t*-test, $P < 0.0001$; saccadic reaction time: 299.5 ± 18.0 ms vs. 203.5 ± 17.8 ms, two-sample *t*-test, $P < 0.0001$), these values were transformed into z-scores for each monkey. We found no significant correlation between the z-scored performance scores or saccadic reaction times and either the within-trial BM index or the DM index (Supplementary Table 1; Pearson's correlation, $r = -0.13–0.15$, $P > 0.14$). These data indicate that the present results cannot be explained simply by session-to-session differences in behavioral performance.

Next, we assessed the effects of eye movements. Although the monkeys were required to fixate on a small spot located at the center of the display throughout the fixation and/or delay period, the eye position window criteria allowed small eye movements, namely microsaccades, within the eye position window. Previous studies have found an association between such small movements and neuronal responses (Martinez-Conde et al. 2004; Gur and Snodderly 2006; Hafed et al. 2009; Hafed and Krauzlis 2010). Therefore, we assessed whether session-to-session variability in small eye movements could lead to a spurious correlation between baseline-activity maintenance and delay-period modulation. We counted the number of small eye movements (absolute eye velocity >

20°/s, duration ≥ 10 ms) during the 800 ms prior to array presentation in the reaction-time task and during the 100–700 ms before the disappearance of the fixation point in the delayed-response task for each of the 94 neurons. In both cases, we observed no correlation between the frequency of small eye movements and the within-trial BM index or the DM index (Supplementary Table 1; Pearson's correlation, r = -0.13–0.08, $P > 0.2$), indicating that the present results could not be explained by small eye movements.

Next, we assessed the effects of anticipation. Baseline activity of LIP neurons can be modulated by anticipation of a behaviorally relevant sensory event and its effects often emerge as ramp-like (build-up) activity prior to the onset of a behaviorally relevant stimulus (Colby et al. 1996). In fact, we observed increasing activity prior to stimulus presentation in some of the neurons we recorded (e.g., Fig. 3*E*). Therefore, it is possible that anticipation strongly modulates baseline and delay-period activity in some neurons, but it only weakly modulates that in other neurons. In such a case, there would be a spurious correlation between baseline-activity maintenance and delay-period modulations across neurons. To test this possibility, we classified our samples into two groups depending on whether neurons exhibited ramp-like activity prior to the time of stimulus onset (Supplementary Fig. 7*A*). Of 94 neurons, 25 exhibited ramp-like activity (25 build-up type neurons and no build-down type neurons). Neither the within-trial BM index nor the DM index significantly differed between the ramping and non-ramping neurons (Supplementary Fig. 7*B*,*C*). Furthermore, the results were essentially the same as those shown in Figure 6*D* even when the ramping neurons were excluded from the partial correlation analysis (Supplementary Fig. 7*D*). Thus, the present results could not be explained by the effects of anticipation.

Next, we assessed the influences of fixation-related activity. Previous studies have reported fixation neurons in the FEF (Bizzi 1968; Suzuki and Azuma 1977; Bruce and Goldberg 1985; Burman and Bruce 1997; Izawa et al. 2009) and the superior colliculus (Munoz and Wurtz 1993; Everling et al. 1998) that are characterized by persistently increasing activity during active

fixation, even during a brief blink of a foveal stimulus, and the cessation of discharge during saccades. Similar fixation-related activity has been found in the LIP (Ben Hamed and Duhamel, 2002). If some of our neurons had such fixation-related activity, it was possible that the values of the within-trial BM and DM indices differed between the fixation-related neurons and the others and this produced a spurious correlation between the BM and DM indices across neurons. Of 94 neurons, only 7 were identified as fixation-related neurons. When the partial correlation analysis was performed after excluding these fixation-related neurons, we still observed essentially the same result as those shown in Figure 6*D* (Supplementary Fig. 8), indicating that the present results could not be explained by the influences of fixation-related activity.

Finally, we considered the possible influences of rhythmic oscillations in baseline activity. A previous study have found that a portion of neurons in area 7a, an adjacent area of LIP, exhibit rhythmic oscillations in their activity even during fixation periods (Joelving et al. 2007). One might argue that if baseline activity rhythmically oscillates at a cycle period on the order of the bin size (100 ms) used for analysis, such oscillations would produce high BM indices. To assess this possibility, we performed a computer simulation in which oscillatory activity was hypothesized, and calculated the within-trial BM indices from this oscillatory activity in the same way as for the actual data (Supplementary Fig. 9). Importantly, the simulation results predict that if oscillatory activity is crucial, there would be not only positive BM indices but also negative BM indices depending on separation time (Supplementary Fig. 9*D*). However, this is inconsistent with our observation that no neuron exhibited the within-trial BM index which was significantly less than zero (Fig. 4*A*). This, it is unlikely that the currently observed high BM indices were produced by rhythmic oscillations in baseline activity.

Effects of neuron type

LIP neurons can be classified into subpopulations based on the existence of visually responsive and/or saccade-burst activity (see Materials and Methods). It is possible that the

correlation between the degree of baseline activity and the strength of delay-period modulations varies depending on neuron type. To test this, we calculated the correlation strength separately for different types of neurons. Of the 94 LIP neurons, 57 (61%), two (2%), and 28 (36%) were classified as visual, movement, and visuomovement neurons, respectively. We found significant partial correlations between within-trial BM and DM indices for visuomovement neurons, factoring out Fano factors, at separation times ranging from 100 to 500 ms (Supplementary Fig. 10; Pearson's partial correlation, $r = 0.42–0.60$, $P < 0.05$). On the other hand, a significant correlation was observed for visual neurons only at a 300-ms separation (Supplementary Fig. 10; Pearson's partial correlation, $r = 0.34$, $P < 0.05$). These results indicate that although the absolute magnitude of correlation coefficients was largely different between the visual and visuomovement neurons, the basic relationship (the longer-term and short-term maintenance of baseline activity complementarily correlated with delay-period modulation and trial-to-trial fluctuations) was preserved irrespective of neuron type.

Relationship to baseline-activity maintenance in other cortical areas

We have previously demonstrated that the degree of baseline-activity maintenance for FEF neurons is significantly stronger than that for V4 neurons, suggesting a difference in the intrinsic temporal storage capability across cortical areas (Ogawa and Komatsu 2010). Although the experimental design and animals used in this study were different from previous studies, it was interesting to compare the mean within-trial BM indices of LIP neurons in the current study with those of FEF (or V4) neurons in our previous study (Supplementary Fig. 11). The results show that the mean within-trial BM indices for LIP neurons ($n = 94$) were significantly lower than those of FEF neurons ($n = 33$) at all separation times (two-sample t-test, $P < 0.001$), but these values were significantly higher than those of V4 neurons ($n = 40$) at all separation times except for 100 ms (two-sample t-test, $P < 0.05$). This result is not contrary to the previously suggested view that the ability to maintain the instantaneous discharge rate in baseline activity increases with the progression in cortical hierarchy (Ogawa and Komatsu 2010).

Discussion

We found that the degree of baseline-activity maintenance during fixation varied from neuron to neuron in the LIP and was significantly correlated with the strength of response modulation signaling task-related information during the delay across neurons. In particular, a significant correlation was observed in the degree of long-term (200–500 ms) baseline-activity maintenance. In contrast, the degree of short-term (~100 ms) baseline-activity maintenance was correlated with trial-to-trial fluctuations evaluated with Fano factors in baseline activity. Thus, the present results suggest that the capability to hold task-related information in delay-period activity is associated with the degree of baseline-activity maintenance in a timescale-dependent manner.

Baseline-activity maintenance during fixation

In this study, we focused on baseline activity during the fixation period to assess the intrinsic ability of a neuron to persistently maintain its discharge rate. This allowed us to examine response properties of LIP neurons under the condition in which the effects of visual sensory stimuli and eye movements may be at a minimum. Although there is the possibility that baseline activity might have been influenced by visually-evoked/saccade-related activity occurring before fixation and/or small eye movements during fixation, our control analyses ruled out these possibilities (Supplementary Fig. 2*A* and Table 1), consistent with our previous study (Ogawa and Komatsu 2010). In addition, although the differences in the within-trial BM indices were significant between the delayed-response and the reaction-time visual search tasks, their differences were very small (Supplementary Fig. 6*A*), suggesting that the preparation to the ongoing task (e.g. Toth and Assad 2002; Stoet and Snyder 2004), if it exists, only weakly influenced on the baseline activity during the fixation period. Finally, behavioural performance had little influence on the degree of baseline-activity maintenance (Supplementary Table 1). Thus, the current results show that the degree of the discharge-rate persistency during the fixation period is very robust irrespective of changes in endogenous or exogenous factors, suggesting that baseline-activity maintenance that we measured in this study may reflect one of the intrinsic response properties of LIP neurons.

Relationship with previous studies of spontaneous activity

Previous studies using functional magnetic resonance imaging techniques have shown that brain regions in which similar blood oxygen level-dependent signal modulations are observed during specific tasks or types of sensory stimulation exhibit correlated spontaneous fluctuations even in the absence of tasks or stimuli (Biswal et al. 1995; Greicius et al. 2003; Fox et al. 2005; Vincent et al. 2007; Northoff et al. 2010), indicating that spontaneous fluctuations in resting state activity manifest an intrinsic functional connectivity (inter-regional correlations in neuronal variability) of the brain. In contrast, the current study focused on single-neuron activity in a particular cortical region and revealed that cell-to-cell functional differences in task-evoked (delay-period) activity are significantly associated with that in baseline activity. Thus, the present results provide new evidence that intrinsic properties characterizing neuronal performance in task-evoked activity could be manifested in spontaneous (baseline) activity at the single-neuron level.

Previous optical imaging studies combined with single-unit recordings have shown that analogous spatial patterns in the cat visual cortex are associated with both stimulus-evoked and spontaneous activities (Arieli et al. 1996; Tsodyks et al. 1999; Kenet et al. 2003). More recently, large-scale multi-unit recording studies found similarly structured patterns of population activity in both stimulus-driven and spontaneous responses of the rat auditory cortex (Curto et al. 2009; Luczak et al. 2009). Furthermore, a single-unit recording study found that spike-time correlations in stimulus-evoked activity are generated by mechanisms common to those operating during spontaneous activity that occurs in the primary visual cortex of anesthetized primates (Jermakowicz et al. 2009). In those studies, the response patterns for stimulus-evoked and spontaneous activity were compared in the absence of any behavioral tasks. In contrast, the present study focused on task-evoked activity (delay-period activity) originating not from sensory stimuli per se but rather from such as memory, attention, and/or motor preparation processes occurring during a behavioral task. Thus, our findings emphasize that intrinsic response properties may reflect not only exogenous

stimulus-driven processing but also endogenous processing at the level of single neurons.

Possible mechanisms for the short- and long-term maintenance of baseline activity

The present results showed that trial-to-trial fluctuations evaluated with Fano factors in baseline activity were more strongly correlated with short-term (~100 ms) baseline-activity maintenance, whereas task-evoked modulation of delay-period activity was more strongly correlated with long-term (200–500 ms) baseline-activity maintenance. What mechanisms could account for the two different time scales of the mechanisms underlying baseline-activity maintenance? It is widely assumed that persistent activity, such as delay-period activity in a memory-guided saccade task, is sustained by the reverberant activation of recurrent excitatory circuits (for reviews see Amit 1995; Wang 2001). Moreover, model studies suggest that not only recurrent circuits but also a slow component of N-methyl-D-aspartate (NMDA) synaptic transmission, which has a decay time constant of about 100 ms (Hestrin et al. 1990; Spruston et al. 1995), play roles in the production of long persistent activity (Wang 1999, 2002).

We speculate that the observed short- and long-term discharge-rate maintenance in baseline activity may be accounted for by these mechanisms. If LIP neurons are equipped with slow-decay NMDA synaptic transmission, they are able to continue receiving excitatory synaptic inputs through NMDA receptors with a decay-time constant of about 100 ms following an action potential; this may explain the potential ability of the neurons to retain their instantaneous discharge rate up to 100 ms. However, because NMDA receptors are broadly distributed over the cerebral cortex (Monaghan and Cotman 1985; Meoni et al. 1998; Scherzer et al. 1998), cell-to-cell variability in the degree of short-term (~100 ms) baseline-activity maintenance may be characterized by the strength of the random fluctuations in input signals. However, if the LIP neurons are also involved in recurrent circuits, they could retain their discharge rate for hundreds of milliseconds or more (Wang 2001). This long persistence may produce not only long-term (200–500 ms) baseline-activity maintenance but also persistent modulation of delay-period activity.

A significant correlation between baseline-activity maintenance in the reaction-time task and delay-period modulation during the delayed-response task (Fig. 6) suggests that persistence in both activities may be produced by shared neural-circuit dynamics. Indeed, a previous *in vitro* study reported that recurrent synaptic reverberation in local neural circuits generates slowly varying spiking patterns in spontaneous activity (Shu et al. 2002) as well as persistent activity during a delay period (Wang 2001). Ganguli et al. (2008) have proposed a theoretical attractor network model that could explain the neuronal behaviors in the LIP during an attentional or perceptual decision-making task. In this model, when feed-forward sensory inputs to the network is absent, population dynamics are assumed to converge on a one-dimensional space in which activity patterns are simply scaled versions of a single pattern of relative firing rates across neurons. This assumption led to the linear relationship between baseline and delay-period activities. They reported that the magnitude of baseline activity is correlated with that of delay-period activity across neurons by examining neurophysiological data recorded from the LIP. In addition to their results, our results demonstrated that temporal structures (discharge-rate persistency) in baseline activity are also correlated with the degree of response modulation of delay-period activity.

Possible functional properties linked with baseline-activity maintenance

The present study demonstrated significant covariance between baseline-activity maintenance and modulation of delay-period activity across LIP neurons. However, this does not mean that a LIP neuron with strong baseline-activity maintenance always exhibited strong modulation in its delay-period activity in the present experiment. Careful inspection of the results of the correlation analysis between the two (e.g., Fig. 6A, 300-ms separation time) revealed that although neurons with weaker baseline-activity maintenance (lower BM indices) tended to have only weaker delay-period modulation (lower DM indices), those with strong baseline-activity maintenance (higher BM indices) appeared to show a range of strengths in delay-period modulation (widely distributed DM indices), demonstrating that some neurons showed strong baseline-activity

maintenance but only weak delay-period modulation during the delayed-response task.

What functional role do these neurons play in the LIP? One possibility is that these neurons play roles in memory-guided actions in which a body part (e.g., arm) other than the eyes is used as the effecter (Snyder et al. 1997; Quian Quiroga et al. 2006; Cui and Andersen 2007). Another possibility is that these neurons play roles in perceptual visual discrimination such as target–distractor discrimination and random dot motion-discrimination tasks (Shadlen and Newsome 2001; Roitman and Shadlen 2002; Ipata et al. 2006; Thomas and Paré 2007; Balan et al., 2008; Ogawa and Komatsu 2009), which require sensory signal integration over time for decision making (Mazurek et al. 2003). A long integration time constant is generally essential for decision making during various perceptual-discrimination tasks. As described above, this can be biophysically achieved using a combination of slow synaptic transmission (possibly dominated by NMDA receptors) and strong network recurrence (Wang 1999, 2002; Shen et al. 2010). Therefore, LIP neurons that had strong baseline-activity maintenance but exhibited only weak delay-period modulation in the present task potentially had the ability to play crucial roles in executing other cognitive tasks that were not assessed in the current experiments.

Funding

This work was supported by grants from the Ministry of Education, Culture, Sports, Science, and Technology of Japan (MEXT) to TO (20500283, 20033010, and 22120507).

Acknowledgments

The authors gratefully acknowledge the continuous support and encouragement of Prof. Kenji Kawano. We also acknowledge Nihon University and the National Bio-Resource Center for supplying the monkeys used in this study. We also thank the editor and anonymous reviewers for their valuable comments and constructive suggestions on the manuscript.

References

Amit DJ. 1995. The Hebbian paradigm reintegrated: local reverberations as internal representations. Behav Brain Sci. 18:617–657.

Andersen RA, Asanuma C, Essick G., Siegel RM. 1990. Corticocortical connections of anatomically and physiologically defined subdivisions within the inferior parietal lobule. J Comp Neurol. 296:65–113.

Arieli A, Sterkin A, Grinvald A, Aertsen A. 1996. Dynamics of ongoing activity: explanation of the large variability in evoked cortical responses. Science. 273:1868–1871.

Balan PF, Oristaglio J, Schneider DM, Gottlieb J. 2008. Neuronal correlates of the set-size effect in monkey lateral intraparietal area. PLoS Biol. 6: e158.

Barash S, Bracewell RM, Fogassi L, Gnadt JW, Andersen RA. 1991a. Saccade-related activity in the lateral intraparietal area. I. Temporal properties; comparison with area 7a. J Neurophysiol. 66:1095–1108.

Barash S, Bracewell RM, Fogassi L, Gnadt JW, Andersen RA. 1991b. Saccade-related activity in the lateral intraparietal area. II. Spatial properties. J Neurophysiol. 66:1109–1124.

Ben Hamed S, Duhamel JR. 2002. Ocular fixation and visual activity in the monkey lateral intraparietal area. Exp Brain Res 142:512-528.

Bisley JW, Goldberg ME. 2003. Neuronal activity in the lateral intraparietal area and spatial attention. Science. 299:81–86.

Bisley JW, Goldberg ME. 2006. Neural correlates of attention and distractibility in the lateral intraparietal area. J Neurophysiol. 95:1696–1717.

Biswal B, Yetkin FZ, Haughton VM, Hyde JS. 1995. Functional connectivity in the motor cortex of resting human brain using echo-planar MRI. Magn Reson Med. 34:537–541.

Bizzi E. 1968. Discharge of frontal eye field neurons during saccadic and following eye movements in unanesthetized monkeys. Exp Brain Res. 6:69–80.

Bruce CJ, Goldberg ME. 1985. Primate frontal eye fields. I. Single neurons discharging before saccades. J Neurophysiol. 53:603–635.

Burman DD, Bruce CJ. 1997. Suppression of task-related saccades by electrical stimulation in the primate's frontal eye field. J Neurophysiol. 77:2252–2267.

Carrasco M, Yeshurun Y. 1998. The contribution of covert attention to the set-size and eccentricity effects in visual search. J Exp Psychol Hum Percept Perform. 24:673–692.

Colby CL, Duhamel JR, Goldberg ME. 1996. Visual, presaccadic, and cognitive activation of single neurons in monkey lateral intraparietal area. J Neurophysiol. 76:2841–2852.

Cui H, Andersen RA. 2007. Posterior parietal cortex encodes autonomously selected motor plans. Neuron. 56:552–559.

Curto C, Sakata S, Marguet S, Itskov V, Harris KD. 2009. A simple model of cortical dynamics explains variability and state dependence of sensory responses in urethane-anesthetized auditory cortex. J Neurosci. 29:10600–10612.

de la Rocha J, Doiron B, Shea-Brown E, Josić K, Reyes A. 2007. Correlation between neural spike trains increases with firing rate. Nature. 448:802–806.

Everling S, Paré M, Dorris MC, Munoz DP. 1998. Comparison of the discharge characteristics of brain stem omnipause neurons and superior colliculus fixation neurons in monkey: implications for control of fixation and saccade behavior. J Neurophysiol. 79:511–528.

Falkner AL, Krishna BS, Goldberg ME. 2010. Surround suppression sharpens the priority map in the lateral intraparietal area. J Neurosci. 30:12787–12797.

Fiser J, Chiu C, Weliky M. 2004. Small modulation of ongoing cortical dynamics by sensory input during natural vision. Nature. 431:573–578.

Fox MD, Raichle ME. 2007. Spontaneous fluctuations in brain activity observed with functional magnetic resonance imaging. Nat Rev Neurosci. 8:700–711.

Fox MD, Snyder AZ, Vincent JL, Corbetta M, Essen DC Van, Raichle ME. 2005. The human brain is intrinsically organized into dynamic, anticorrelated functional networks. Proc Natl Acad Sci U S A. 102:9673–9678.

Fuchs AF, Robinson DA. 1966. A method for measuring horizontal and vertical eye movement chronically in the monkey. J Appl Physiol. 21:1068–1070.

Ganguli S, Bisley JW, Roitman JD, Shadlen MN, Goldberg ME, Miller KD. 2008. One-dimensional dynamics of attention and decision making in LIP. Neuron. 58:15–25.

Gifford GW 3rd, Cohen YE. 2004, Effect of a central fixation light on auditory spatial responses in area LIP. J Neurophysiol. 91:2929–2933.

Gnadt JW, Andersen RA. 1988. Memory related motor planning activity in posterior parietal cortex of macaque. Exp Brain Res. 70:216–220.

Greicius M. 2008. Resting-state functional connectivity in neuropsychiatric disorders. Curr Opin Neurol. 21:424–430.

Greicius MD, Krasnow B, Reiss AL, Menon V. 2003. Functional connectivity in the resting brain: a network analysis of the default mode hypothesis. Proc Natl Acad Sci U S A. 100:253–258.

Gur M, Snodderly DM. 2006. High response reliability of neurons in primary visual cortex (V1) of alert, trained monkeys. Cereb Cortex. 16:888–895.

Hafed ZM, Goffart L, Krauzlis RJ. 2009. A neural mechanism for microsaccade generation in the primate superior colliculus. Science. 323:940–943.

Hafed ZM, Krauzlis RJ. 2010. Microsaccadic suppression of visual bursts in the primate superior colliculus. J Neurosci. 30:9542–9547.

Hestrin S, Sah P, Nicoll RA. 1990. Mechanisms generating the time course of dual component excitatory synaptic currents recorded in hippocampal slices. Neuron. 5:247–253.

Hikosaka O, Wurtz RH. 1983. Visual and oculomotor functions of monkey substantia nigra pars reticulata. III. Memory-contingent visual and saccade responses. J Neurophysiol. 49:1268–1284.

Ipata AE, Gee AL, Goldberg ME, Bisley JW. 2006. Activity in the lateral intraparietal area predicts the goal and latency of saccades in a free-viewing visual-search task. J Neurosci. 26:3656–3661.

Izawa Y, Suzuki H, Shinoda Y. 2009. Response properties of fixation neurons and their location in the frontal eye field in the monkey. J Neurophysiol. 102:2410–2422.

Jermakowicz WJ, Chen X, Khaytin I, Bonds AB, Casagrande VA. 2009. Relationship between

spontaneous and evoked spike-time correlations in primate visual cortex. J Neurophysiol. 101:2279–2289.

Joelving FC, Compte A, Constantinidis C. 2007. Temporal properties of posterior parietal neuron discharges during working memory and passive viewing. J Neurophysiol. 97:2254–2266.

Judge SJ, Richmond BJ, Chu FC. 1980. Implantation of magnetic search coils for measurement of eye position: an improved method. Vis Res. 20:535–538.

Kenet T, Bibitchkov D, Tsodyks M, Grinvald A, Arieli A. 2003. Spontaneously emerging cortical representations of visual attributes. Nature. 425:954–956.

Kobayashi Y, Inoue Y, Yamamoto M, Isa T, Aizawa H. 2002. Contribution of pedunculopontine tegmental nucleus neurons to performance of visually guided saccade tasks in monkeys. J Neurophysiol. 88:715–731.

Lawrence BM, White RL, Snyder LH. 2005. Delay-period activity in visual, visuomovement, and movement neurons in the frontal eye field. J Neurophysiol. 94:1498–1508.

Linden JF, Grunewald A, Andersen RA. 1999. Responses to auditory stimuli in macaque lateral intraparietal area. II. Behavioral modulation. J Neurophysiol. 82:343–358.

Luczak A, Barthó P, Harris KD. 2009. Spontaneous events outline the realm of possible sensory responses in neocortical populations. Neuron. 62:413–425.

Maimon G, Assad JA. 2006. A cognitive signal for the proactive timing of action in macaque LIP. Nat Neurosci. 9:948–955.

Martinez-Conde S, Macknik SL, Hubel DH. 2004. The role of fixational eye movements in visual perception. Nat Rev Neurosci. 5:229–240.

Mazurek ME, Roitman JD, Ditterich J, Shadlen MN. 2003. A role for neural integrators in perceptual decision making. Cereb Cortex. 13:1257–1269.

Meinecke C, Donk M. 2002. Detection performance in pop-out tasks: nonmonotonic changes with display size and eccentricity. Perception. 31:591–602.

Meoni P, Bunnemann BH, Trist DG, Bowery NG. 1998. N-terminal splice variants of the NMDAR1 glutamate receptor subunit: differential expression in human and monkey brain. Neurosci Lett.

249:45–48.

Monaghan DT, Cotman CW. 1985. Distribution of N-methyl-D-aspartate-sensitive L-[3H]glutamate-binding sites in rat brain. J Neurosci. 5:2909–2919.

Mountcastle VB, Lynch JC, Georgopoulos A, Sakata H, Acuna C. 1975. Posterior parietal association cortex of the monkey: command functions for operations within extrapersonal space. J Neurophysiol. 38:871–908.

Munoz DP, Wurtz RH. 1993. Fixation cells in monkey superior colliculus. I. Characteristics of cell discharge. J Neurophysiol. 70:559–575.

Northoff G, Qin P, Nakao T. 2010. Rest–stimulus interaction in the brain: a review. Trends Neurosci. 33:277–284.

Ogawa T, Komatsu H. 2009. Condition-dependent and condition-independent target selection in the macaque posterior parietal cortex. J Neurophysiol. 101:721–736.

Ogawa T, Komatsu H. 2010. Differential temporal storage capacity in the baseline activity of neurons in macaque frontal eye field and area V4. J Neurophysiol. 103:2433–2445.

Okada K, Toyama K, Inoue Y, Isa T, Kobayashi Y. 2009. Different pedunculopontine tegmental neurons signal predicted and actual task rewards. J Neurosci. 29:4858–4870.

Petersch B, Bogner J, Fransson A, Lorang T, Pötter R. 2004. Effects of geometric distortion in 0.2 T MRI on radiotherapy treatment planning of prostate cancer. Radiother Oncol. 71**:**55–64.

Petersen CCH, Hahn TTG, Mehta M, Grinvald A, Sakmann B. 2003. Interaction of sensory responses with spontaneous depolarization in layer 2/3 barrel cortex. Proc Natl Acad Sci U S A. 100:13638–13643.

Quian Quiroga R, Snyder LH, Batista AP, Cui H, Andersen R. 2006. Movement intention is better predicted than attention in the posterior parietal cortex. J Neurosci. 26:3615–3620.

Richmond BJ, Optican LM. 1990. Temporal encoding of two-dimensional patterns by single units in primate primary visual cortex. II. Information transmission. J Neurophysiol. 64:370–380.

Ringach DL. 2009. Spontaneous and driven cortical activity: implications for computation. Curr Opin Neurobiol. 19:439–444.

Roitman JD, Shadlen MN. 2002. Response of neurons in the lateral intraparietal area during a combined visual discrimination reaction time task. J Neurosci. 22:9475–9489.

Sakata S, Harris KD. 2009. Laminar structure of spontaneous and sensory-evoked population activity in auditory cortex. Neuron. 64:404–418.

Scherzer CR, Landwehrmeyer GB, Kerner JA, Counihan TJ, Kosinski CM, Standaert DG, Daggett LP, Veliçelebi G, Penney JB, Young AB. 1998. Expression of N-methyl-D-aspartate receptor subunit mRNAs in the human brain: hippocampus and cortex. J Comp Neurol. 390:75–90.

Shadlen MN, Newsome WT. 2001. Neural basis of a perceptual decision in the parietal cortex (area LIP) of the rhesus monkey. J Neurophysiol. 86:1916–1936.

Shen K, Kalwarowsky S, Clarence W, Brunamonti E, Paré M. 2010. Beneficial effects of the NMDA antagonist ketamine on decision processes in visual search. J Neurosci. 30:9947–9953.

Shu Y, Hasenstaub A, McCormick DA. 2003. Turning on and off recurrent balanced cortical activity. Nature. 423:288–293.

Snyder LH, Batista AP, Andersen RA. 1997. Coding of intention in the posterior parietal cortex. Nature. 386:167–170.

Spruston N, Jonas P, Sakmann B. 1995. Dendritic glutamate receptor channels in rat hippocampal CA3 and CA1 pyramidal neurons. J Physiol. 482:325–352.

Stoet G, Snyder LH. 2004. Single neurons in posterior parietal cortex of monkeys encode cognitive set. Neuron. 42:1003–1012.

Suzuki H, Azuma M, Yumiya H. 1979. Stimulus and behavioral factors contributing to the activation of monkey prefrontal neurons during gazing. Jpn J Physiol. 29:471–489.

Thomas NWD, Paré M. 2007. Temporal processing of saccade targets in parietal cortex area LIP during visual search. J Neurophysiol. 97:942–947.

Toth LJ, Assad JA. 2002. Dynamic coding of behaviourally relevant stimuli in parietal cortex. Nature. 415:165–168.

Tsodyks M, Kenet T, Grinvald A, Arieli A. 1999. Linking spontaneous activity of single cortical neurons and the underlying functional architecture. Science. 286:1943–1946.

Vincent JL, Patel GH, Fox MD, Snyder AZ, Baker JT, Essen DC Van, Zempel JM, Snyder LH, Corbetta M, Raichle ME. 2007. Intrinsic functional architecture in the anaesthetized monkey brain. Nature. 447:83–6l.

Wang XJ. 1999. Synaptic basis of cortical persistent activity: the importance of NMDA receptors to working memory. J Neurosci. 19:9587–9603.

Wang XJ. 2001. Synaptic reverberation underlying mnemonic persistent activity. Trends Neurosci. 24:455–463.

Wang XJ. 2002. Probabilistic decision making by slow reverberation in cortical circuits. Neuron. 36:955–968.

Wolfe JM, O'Neill P, Bennett SC. 1998. Why are there eccentricity effects in visual search? Visual and attentional hypotheses. Percept Psychophys. 60:140–156.

Figure legends

Figure 1. Visual stimuli and behavioral tasks. (*A*) Delayed-response visual-search task. After fixation for typically 1,000 ms, either an isolated target stimulus or a color-singleton target embedded in a search array was presented for 500 or 700 ms. The fixation spot disappeared after a variable delay (800–1,800 ms), and the monkeys had to make a saccade (arrow) toward the location at which the target had appeared. The monkeys received a juice reward following an additional fixation at the target location (600 ms). (*B*) Reaction-time visual-search task. The procedure was the same as that in the delayed-response task except that no artificial delay was imposed. The ongoing task was cued by the color or shape of the fixation spot (yellow circle or white rectangle, delayed-response task; white circle, reaction-time task). In particular, we focused on baseline activity during the fixation period in the reaction-time task and on task-evoked activity during the delay period in the delayed-response task (thick frames).

Figure 2. Magnetic resonance images of recording sites from one monkey. (*A*) A three-dimensional view of the brain. The five bright rods in the right hemisphere indicate tubes filled with a glycerin solution and embedded in a plastic base attached to the recording chamber. These tubes served as position reference markers. The bright mass located at the foot of the tubes is ointment with which a hole in the skull was filled to protect the dura matter surface. (*B*) Penetration sites on the cortical surface. Large circles indicate the sites defined by extensions from the reference tubes. The penetration sites where neurons were recorded were reconstructed with the coordinates determined by the reference tubes. (*C*) The number of neurons that were recorded within each grid location. The thick gray line indicates the location of the IPS. (*D*) Reconstruction of the recording zone in the planes that were sectioned parallel to the penetrations at two levels. *D*a and *D*b correspond to the planes sectioned at lines a and b in *B*, respectively. The arrowheads next to IPS represent the boundaries of the locations from which neurons were recorded. (*E*) Coronal slices representing the most anterior to the most posterior recording positions. The A-P levels are indicated in the upper

center of each image. CS, central sulcus; IPS, intraparietal sulcus.

Figure 3. Baseline-activity maintenance and delay-period modulation in single LIP neurons. (*A*–*E*) A neuron exhibiting strong baseline-activity maintenance. (*A*) Activity (mean ± SE) during the reaction-time visual-search task. The fixation period was set at 1,000 ms during the recording session of this neuron. Left and right vertical dashed lines indicate fixation onset and stimulus onset, respectively. The gray rectangle indicates the interval used for data analysis. (*B*) Spike-density functions of the high- (red), medium- (green), and low-activity (blue) groups classified according to the spike count during a 100-ms interval (gray rectangle) during the fixation period. Vertical tick marks indicate action potentials, and each row of rasters indicates one trial. Only the first 20 trials are shown for each group for clarity. The horizontal line indicates the interval during which the high- and low-activity traces differed significantly (Mann–Whitney *U*-test, $P < 0.01$). (*C*) Within-trial (circles) and across-trial (squares) BM indices plotted as a function of separation time. Black symbols indicate that the index values are significantly different from zero (Pearson's correlation, $P < 0.01$). (*D*) Activity during the delayed-response visual-search task when an isolated target fell inside (black trace) or outside (gray trace) the receptive field. Vertical dashed lines indicate the target onset (left), target offset (middle), and fixation spot disappearance (right). Gray rectangle indicates the interval used for data analysis. (*E*–*H*) Another LIP neuron exhibiting weak baseline-activity maintenance. Conventions are the same as those used in *A*–*D*.

Figure 4. Population analysis of baseline-activity maintenance. (*A*) Within-trial BM indices from 94 LIP neurons. Circles connected with a thin gray line represent the BM indices for each neuron. The thick black line indicates the population average. Black circles indicate that the index values differed significantly from zero (Pearson's correlation, $P < 0.01$). Data corresponding to the example neurons (Fig. 3) are indicated by highlighted lines. (*B*) Across-trial BM indices for 94 neurons. Conventions are the same as those used in *A*.

Figure 5. Population analysis of delay-period modulation. (*A*) Distribution of DM indices for 94 LIP neurons. The gray bars indicate the neurons exhibiting significant target location-dependent modulation of delay-period response (Mann–Whitney *U*-test, $P < 0.05$). (*B–D*) Spike-density functions (mean [thick trace] ± SE [thin trace]) during the delayed-response visual-search task calculated separately from the three subpopulations into which 94 neurons were divided based on the strength of the DM index: high- (*B*), middle- (*C*), and low-DM (*D*) indices, respectively. Conventions are the same as those used in Figure 3*D*.

Figure 6. Timescale-dependent correlations of delay-period modulation and Fano factors with baseline-activity maintenance. (*A*) Relationship between DM and within-trial BM indices for 94 neurons. The BM indices used here were calculated from spike counts of bins separated by intervals of 100 ms (left), 300 ms (middle), and 500 ms (right). Circles represent individual neurons. Lines indicate the least-squares fit to the data when the correlations were significant (Pearson's correlation, $P < 0.05$). (*B*) Relationship between Fano factors and within-trial BM indices for 94 neurons. (*C*) Raw correlation coefficients between within-trial BM and DM indices (black bars) and between within-trial BM indices and Fano factors (gray bars) are plotted as a function of separation time used to calculate the BM index. (*D*) Partial correlation coefficients between within-trial BM and DM indices factoring out Fano factors (black bars) and those between within-trial BM indices and Fano factors factoring out DM indices (gray bars). $^{***}P < 0.001$, $^{**}P < 0.01$, $^{*}P < 0.05$.

Figure 7. Partial correlations among within-trial BM indices, DM indices, and Fano factors calculated for various combinations of separation time and bin width. (*A*) Heat map of partial correlation coefficients between within-trial BM and DM indices factoring out Fano factors. Pairs of separation times (10–790 ms in 10-ms steps) and bin widths (40–400 ms in 10-ms steps) were chosen so that two bins were not overlapped and that they did not exceed the analytic interval (800 ms). (*B*) Heat map of partial correlation coefficients between within-trial BM indices and Fano factors factoring out DM indices.

Figure 1

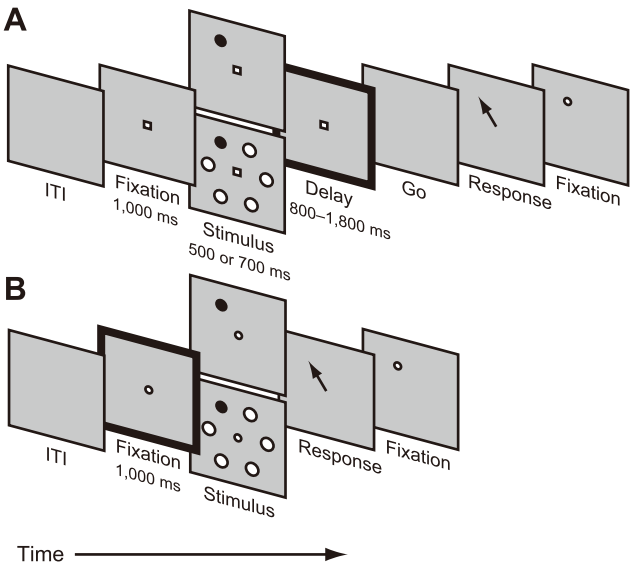
A
ITI
Fixation
1,000 ms
Stimulus
500 or 700 ms
Delay
800~1,800 ms
Go
Response
Fixation
B
ITI
Fixation
1,000 ms
Stimulus
Response
Fixation
Time

Figure 2

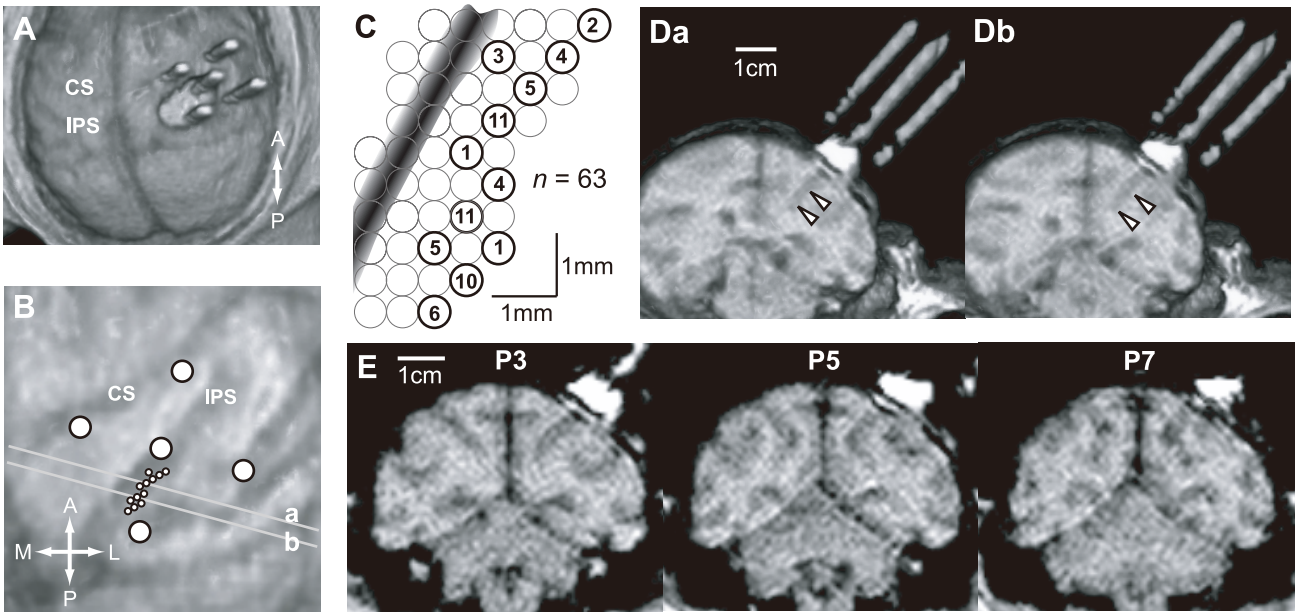
A
CS
IPS
A
P
B
CS
IPS
A
M
L
P
a
b
C
2
3
4
5
11
1
4
11
5
1
10
6
n = 63
1mm
1mm
Da
1cm
Db
E
1cm
P3
P5
P7

Figure 3

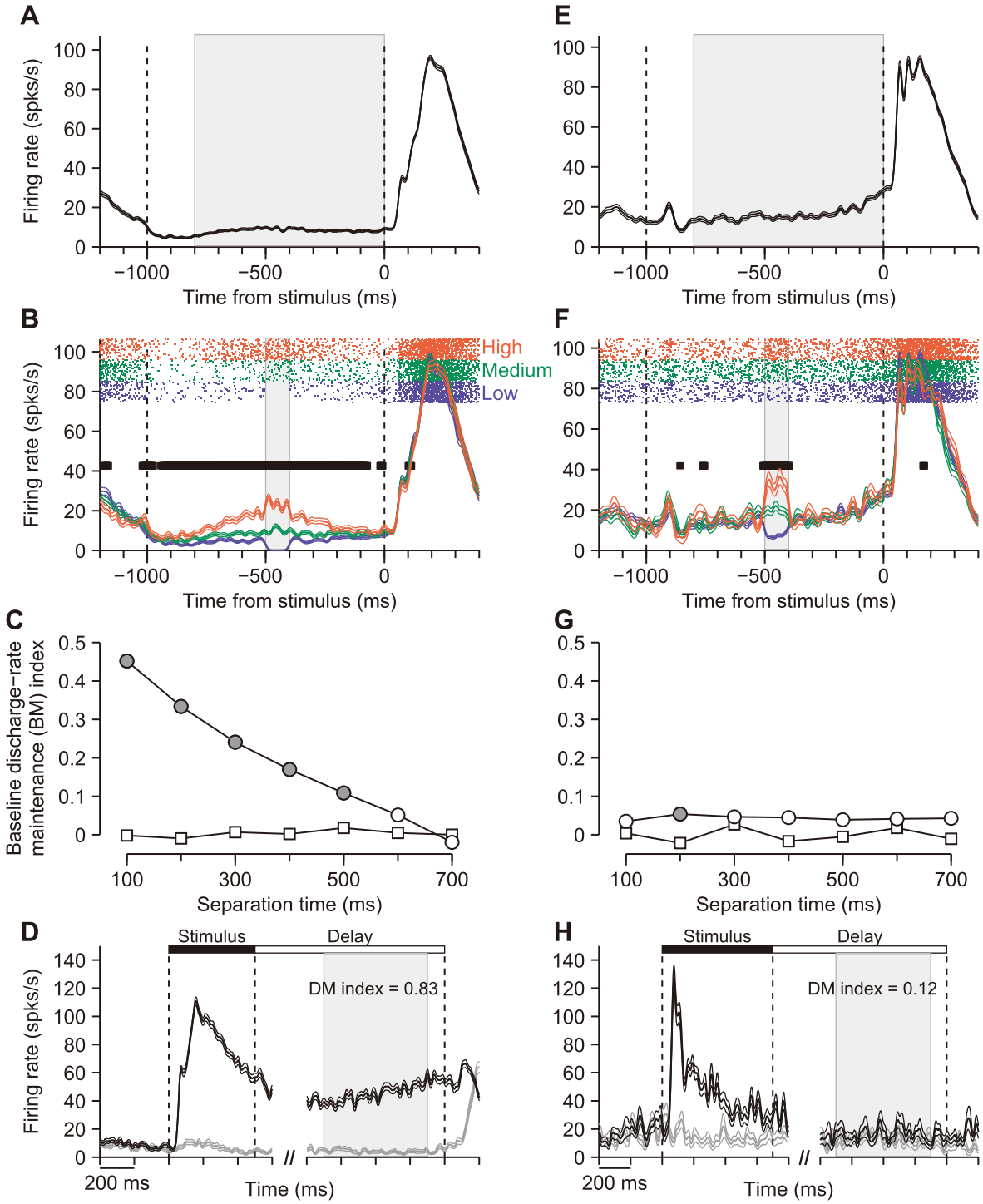
A
E
B
F
C
G
D
H
Firing rate (spks/s)
Time from stimulus (ms)
High
Medium
Low
Baseline discharge-rate maintenance (BM) index
Separation time (ms)
Stimulus
Delay
DM index = 0.83
DM index = 0.12
200 ms
Time (ms)

Figure 4

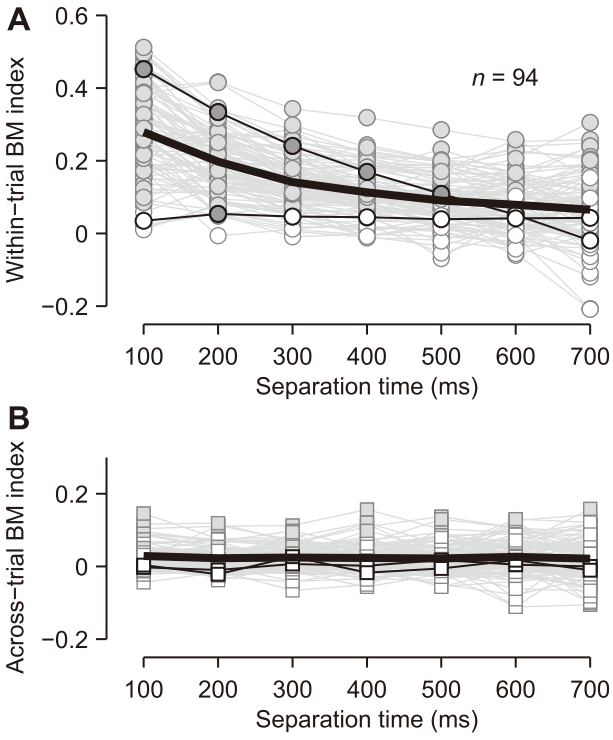
A
Within−trial BM index
0.6
0.4
0.2
0
−0.2
n = 94
100
200
300
400
500
600
700
Separation time (ms)
B
Across−trial BM index
0.2
0
−0.2
100
200
300
400
500
600
700
Separation time (ms)

Figure 5

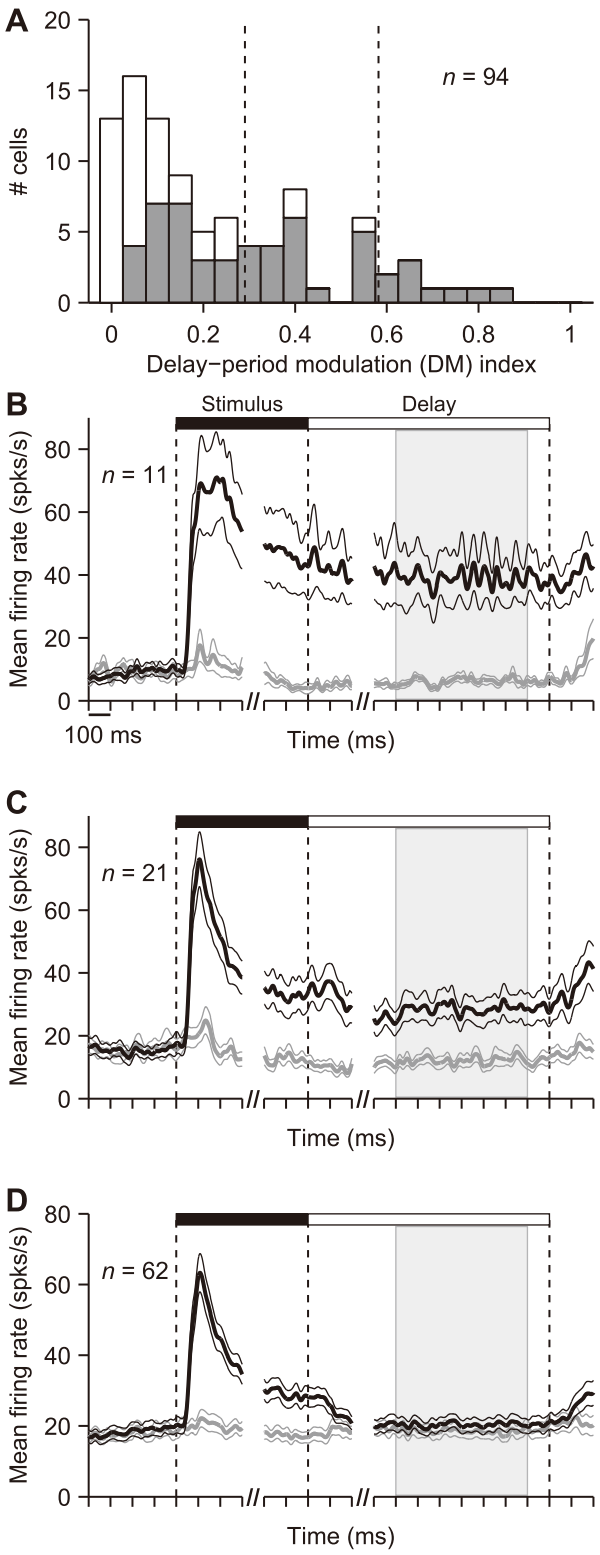
A
20
15
10
5
0
# cells
n = 94
0
0.2
0.4
0.6
0.8
1
Delay−period modulation (DM) index
B
Stimulus
Delay
n = 11
Mean firing rate (spks/s)
80
60
40
20
0
100 ms
Time (ms)
C
n = 21
Mean firing rate (spks/s)
Time (ms)
D
n = 62
Mean firing rate (spks/s)
Time (ms)

Figure 6

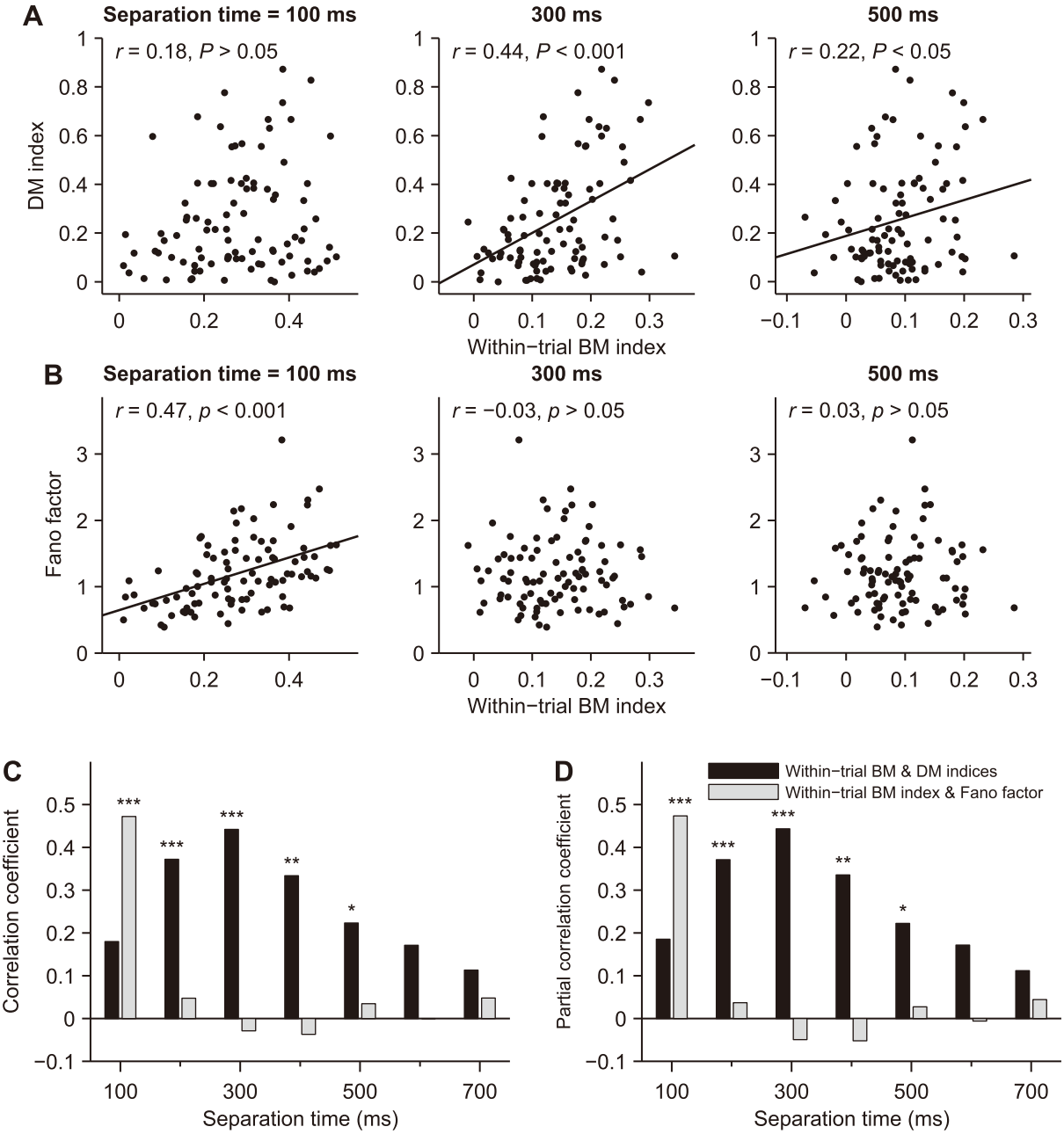
A
Separation time = 100 ms
r = 0.18, P > 0.05
300 ms
r = 0.44, P < 0.001
500 ms
r = 0.22, P < 0.05
DM index
Within−trial BM index
B
Separation time = 100 ms
r = 0.47, p < 0.001
300 ms
r = −0.03, p > 0.05
500 ms
r = 0.03, p > 0.05
Fano factor
Within−trial BM index
C
Correlation coefficient
Separation time (ms)
D
Within−trial BM & DM indices
Within−trial BM index & Fano factor
Partial correlation coefficient
Separation time (ms)

Figure 7

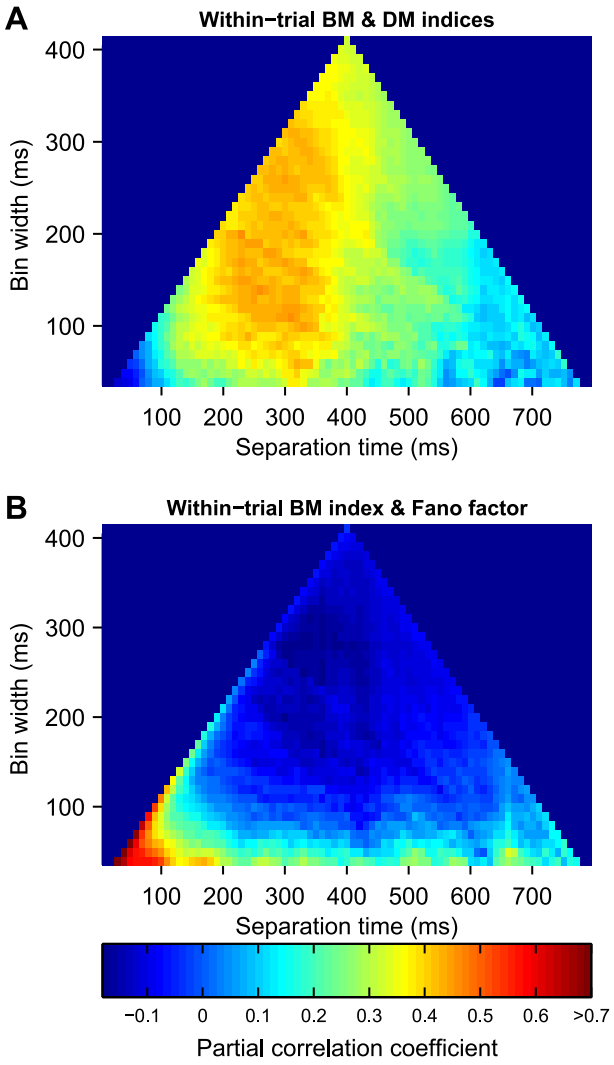
A
Within−trial BM & DM indices
Bin width (ms)
400
300
200
100
100 200 300 400 500 600 700
Separation time (ms)
B
Within−trial BM index & Fano factor
Bin width (ms)
400
300
200
100
100 200 300 400 500 600 700
Separation time (ms)
−0.1 0 0.1 0.2 0.3 0.4 0.5 0.6 >0.7
Partial correlation coefficient

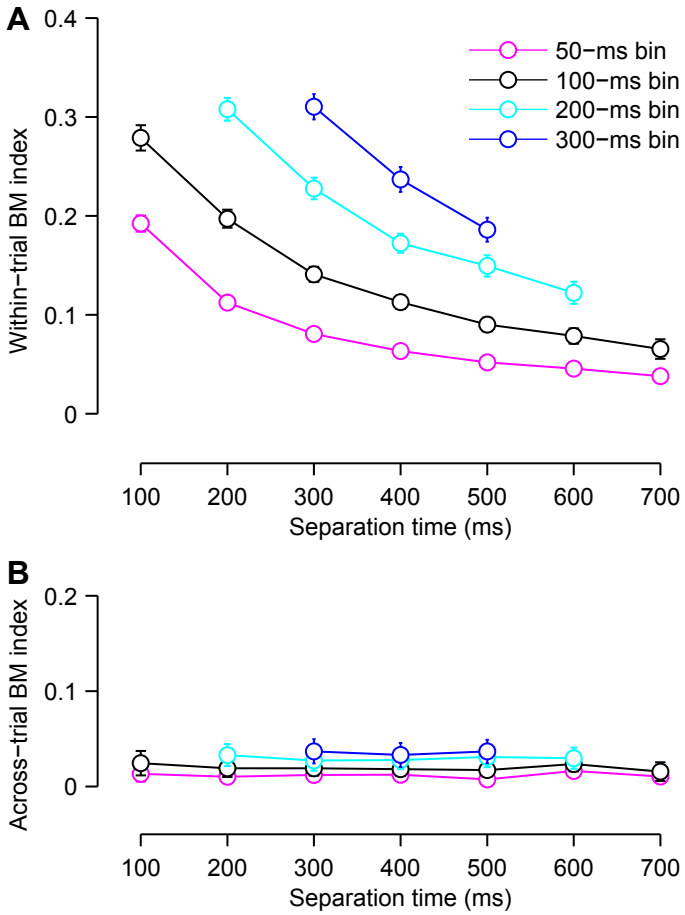

Supplementary Figure 1. Within-trial (*A*) and across-trial BM indices (*B*) evaluated using a different bin width of 50 (magenta), 100 (black), 200 (cyan), or 300 ms (blue). Circles connected by lines indicate averaged indices across 94 LIP neurons (mean ± *SE*). The within-trial BM indices for all bin widths decreased as separation time increased (Spearman's correlation, ρ = -0.57, -0.50, and -0.39 for bin widths of 50, 200, and 300 ms, respectively, $P < 0.0001$). In addition, the across-trial BM indices for all bin widths were close to zero irrespective of separation time.

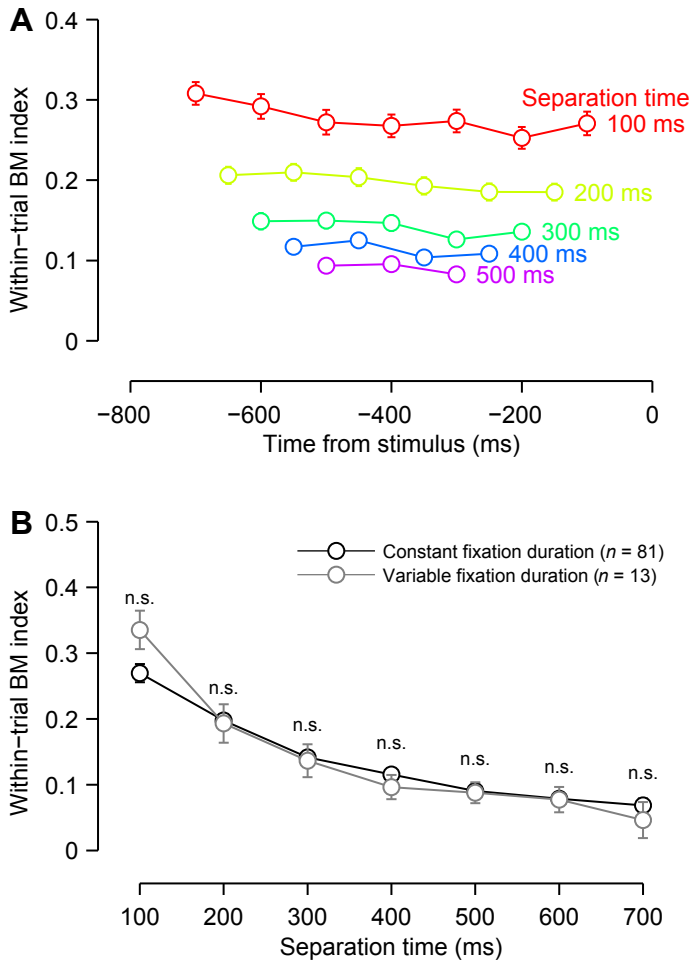

Supplementary Figure 2. Stability of the within-trial BM index. (*A*) The BM indices (mean ± SE) across 94 neurons as a function of time before the array presentation. Each BM index was calculated from a pair of 100-ms bins in 100-ms steps within the 800-ms period preceding array presentation. A pair of bins were temporally separated by either 100, 200, 300, 400, or 500 ms. Each data point is plotted at the mean time of two time bins used to calculate the index. Circles connected by a colored line represent the BM indices obtained from the same separation time (100–500 ms). Although the BM indices at separation times ranging from 100 to 300 ms significantly varied across the fixation time (one-way repeated-measures analysis of variance, $P < 0.05$), their changes were rather small and the overall tendency of a gradual decrease in the BM index with an increase in separation time was stable throughout the fixation period. (*B*) Influences of fixation time. In the recordings, the length of the fixation period was fixed (1,000 ms) for most LIP cells, but it was variable (1,500–2,000 ms) for a minority of cells. To test the possibility whether the difference in fixation time produced any difference in the degree of baseline-activity maintenance, we divided neurons into two groups according to whether the fixation duration was constant (black; $n = 81$) or variable (gray; $n = 13$) and computed the within-trial BM indices separately for each neuron group. Each data point shows the mean (± SE) BM index for each group. No significant difference was observed in the BM indices at all separation times (two-sample *t*-test, $P > 0.07$).

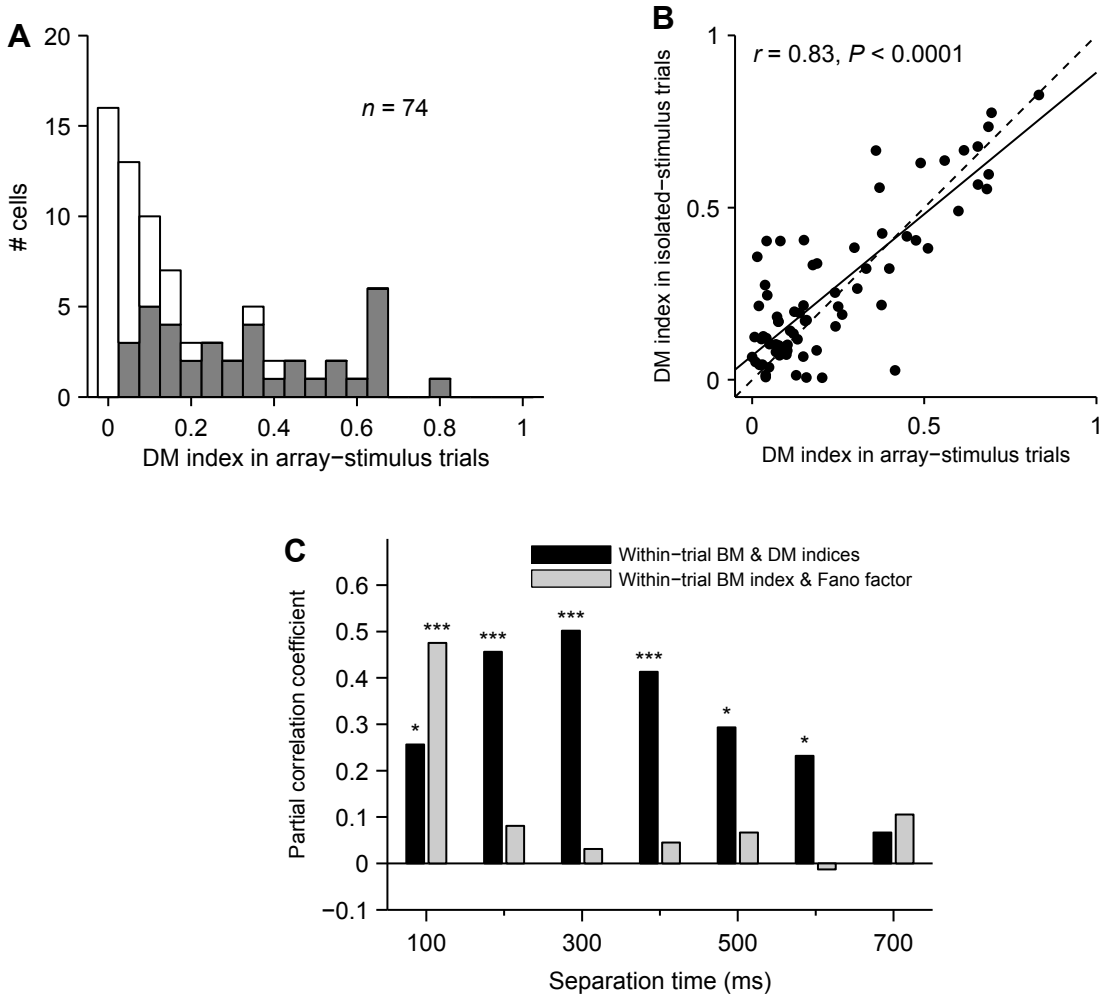

Supplementary Figure 3. DM index derived from the array-stimulus trials. Delay-period activity was examined with the array-stimulus trials for 74 neurons. (*A*) Distribution of the DM indices derived from delay-period activity in the array-stimulus trials (0–0.83, mean ± *SD* = 0.23 ± 0.22). Gray bars indicate neurons with significant target direction-dependent modulations in the delay (37/74 = 50%; Mann–Whitney *U*-test, $P < 0.05$). (*B*) The DM indices calculated from the array-stimulus and isolated-stimulus trials were compared for the 74 neurons. Circles represent individual neurons. The dashed and solid lines indicate the unity line and the least-squares fit to the data, respectively. A strong correlation was found between these two index values (Pearson's correlation, $r = 0.83$, $P < 0.0001$). (*C*) The partial correlation analysis performed using the DM indices from the array-stimulus trials for the 74 neurons. Black bars indicate partial correlation coefficients between within-trial BM and DM indices factoring out Fano factors, and gray bars indicate those between within-trial BM indices and Fano factors factoring out DM indices. ***$P < 0.001$, **$P < 0.01$, *$P < 0.05$.

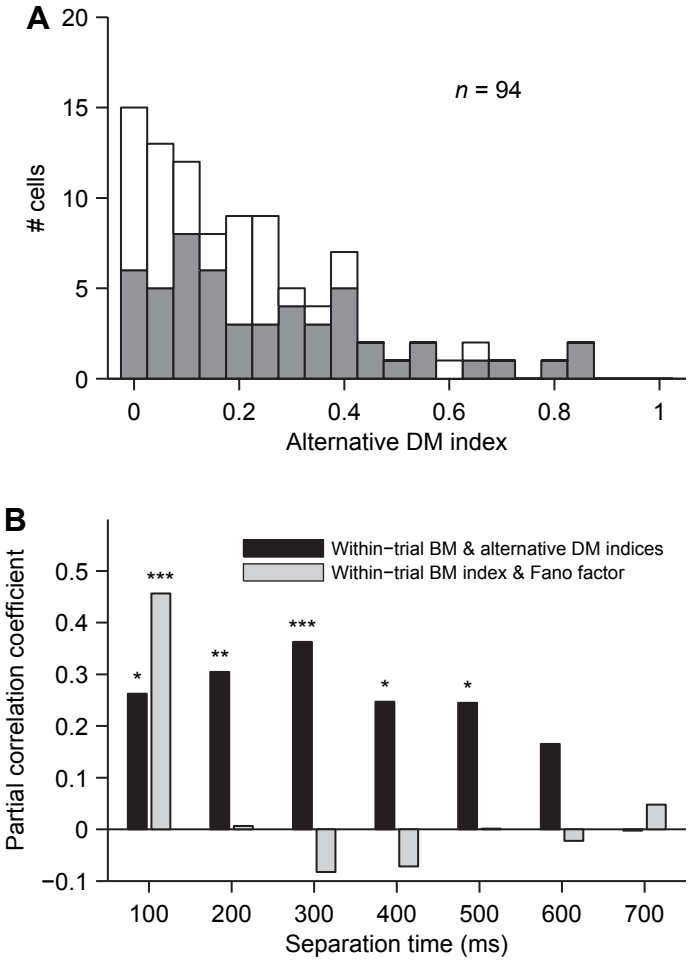

Supplementary Figure 4. Alternative measurement for delay-period modulation. For each neuron, we computed an alternative measurement for delay-period modulation in which the mean discharge rate during trials in which the target appeared inside the receptive field was compared with the baseline discharge rate. This alternative DM index was defined as $|R_{delay} – R_{prestim}|/(R_{delay} + R_{prestim})$, where R_{delay} and $R_{prestim}$ refer to the mean discharge rate during the delay period (a 600-ms interval from 100 to 700 ms before the disappearance of the fixation spot) and that during the prestimulus period (a 200-ms interval before array presentation) of trials in which the target appeared inside the receptive field, respectively. (*A*) Distribution of the alternative DM indices. (0–0.90, mean ± SD = 0.24 ± 0.21). Gray bars indicate neurons with significant target direction-dependent modulations in the delay. (*B*) The partial correlation analysis performed using the alternative DM indices. Same conventions as in Supplementary Figure 3*C*.

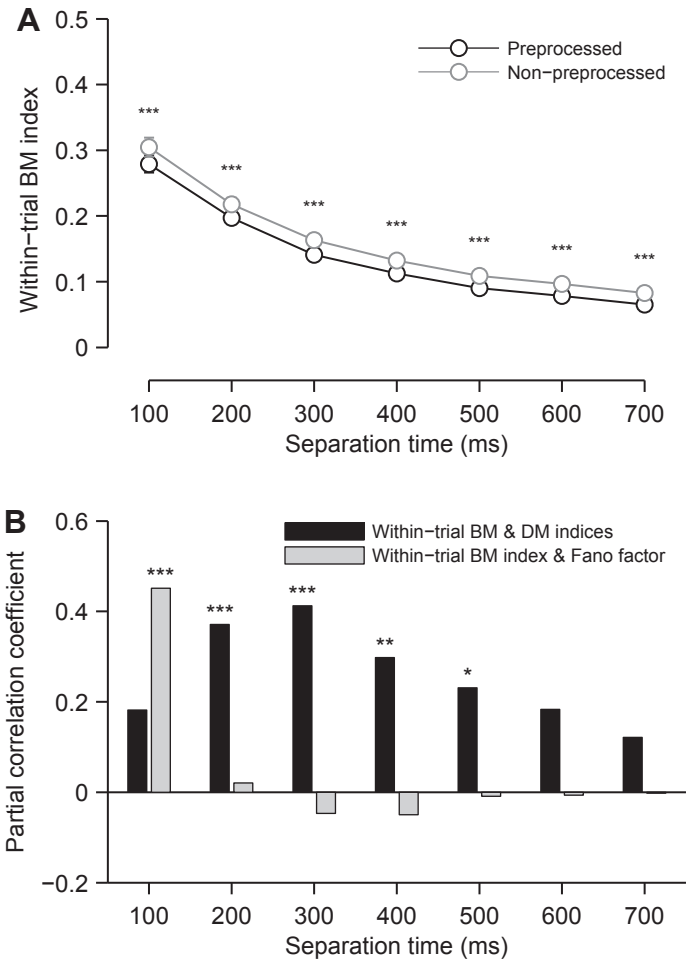

Supplementary Figure 5. Influences of a data preprocessing step for removing trials with slow drifts in baseline activity. (A) Comparison of the within-trial BM indices obtained from trials that were preprocessed (black) or non-preprocessed (gray). There was a little but significant difference at all separation times (paired *t*-test, $P < 0.001$). (B) Partial correlations of the DM index and Fano factor with the within-trial BM index, when the data preprocessing was not performed. Same conventions as in Supplementary Figure 3*C*.

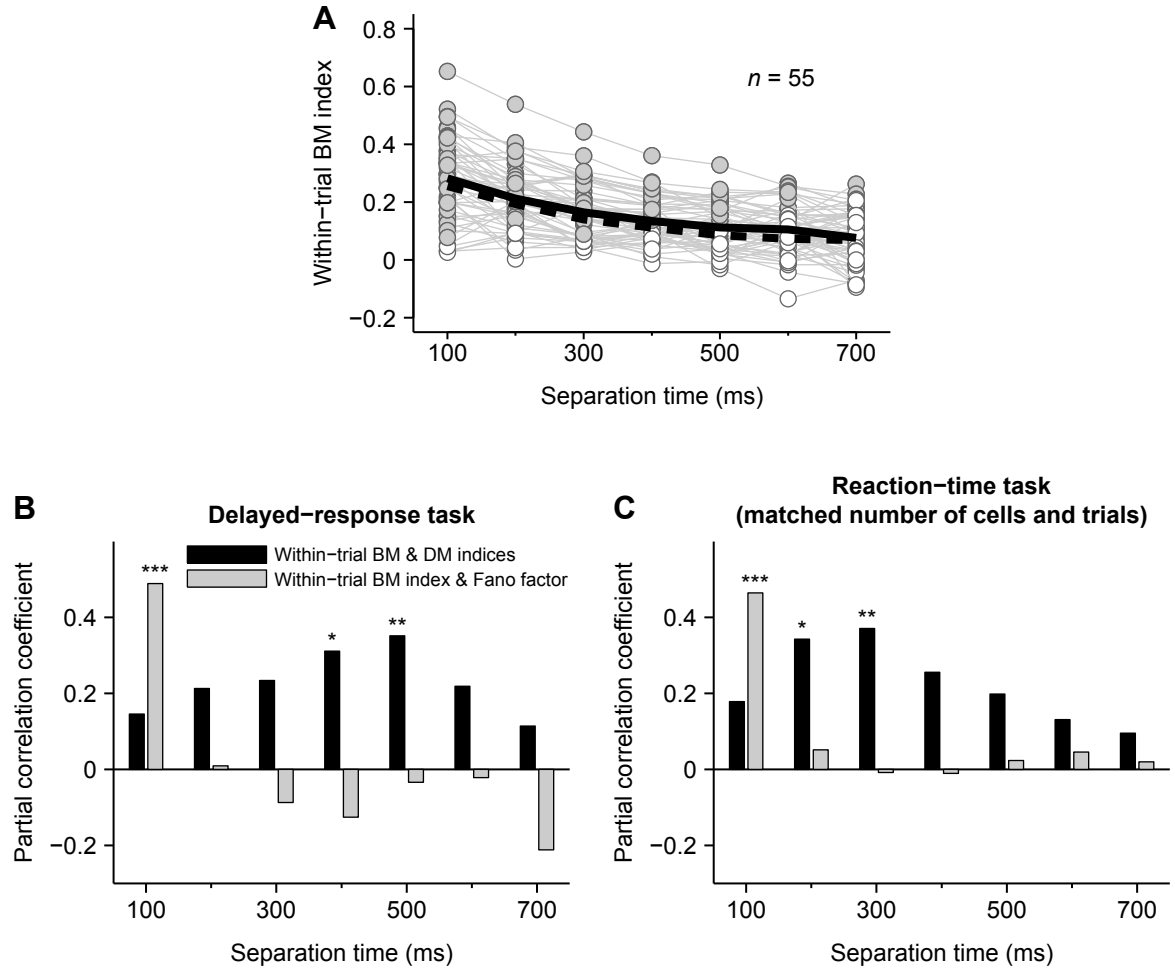

Supplementary Figure 6. BM index derived from the baseline activity during the delayed-response task. (*A*) Within-trial BM indices evaluated from the baseline activity in the delayed-response task. The indices were derived from 55 cells that fulfilled the criteria for appreciable baseline activity (≥5 spikes/s, 5.2–45.8 spikes/s, mean ± *SD* = 15.1 ± 8.2 spikes/s) and sufficient trials (≥100 trials, 102–574 trials, mean ± *SD* = 163 ± 77 trials). The mean values of the within-trial BM indices were significantly different between the delayed-response task (thick solid line) and the reaction-time task (thick dashed line) at all separation times except 200 ms (paired *t*-test, $P < 0.05$). However, the differences were very small, and the dependence of the within-trial BM indices on separation time was quite similar between the two task conditions. Conventions are the same as those used in Figure 4*A*. (*B*) Partial correlations of the DM index and Fano factor with the within-trial BM index measured in the delayed-response task. (*C*) Simulated partial correlations of the DM index and Fano factor with the within-trial BM index measured in the reaction-time task. We randomly selected neurons and their trial data so that the number of cells and trials were matched to those in the delayed-response task (*B*) with a bootstrap method. Using this data set, a set of partial correlation coefficients was calculated in the same way as for the actual data. After repeating this procedure 1000 times, the simulated partial correlations were obtained by averaging the 1000 sets of partial correlation coefficients. Conventions in *B* and *C* are the same as those used in Supplementary Figure 3*C*.

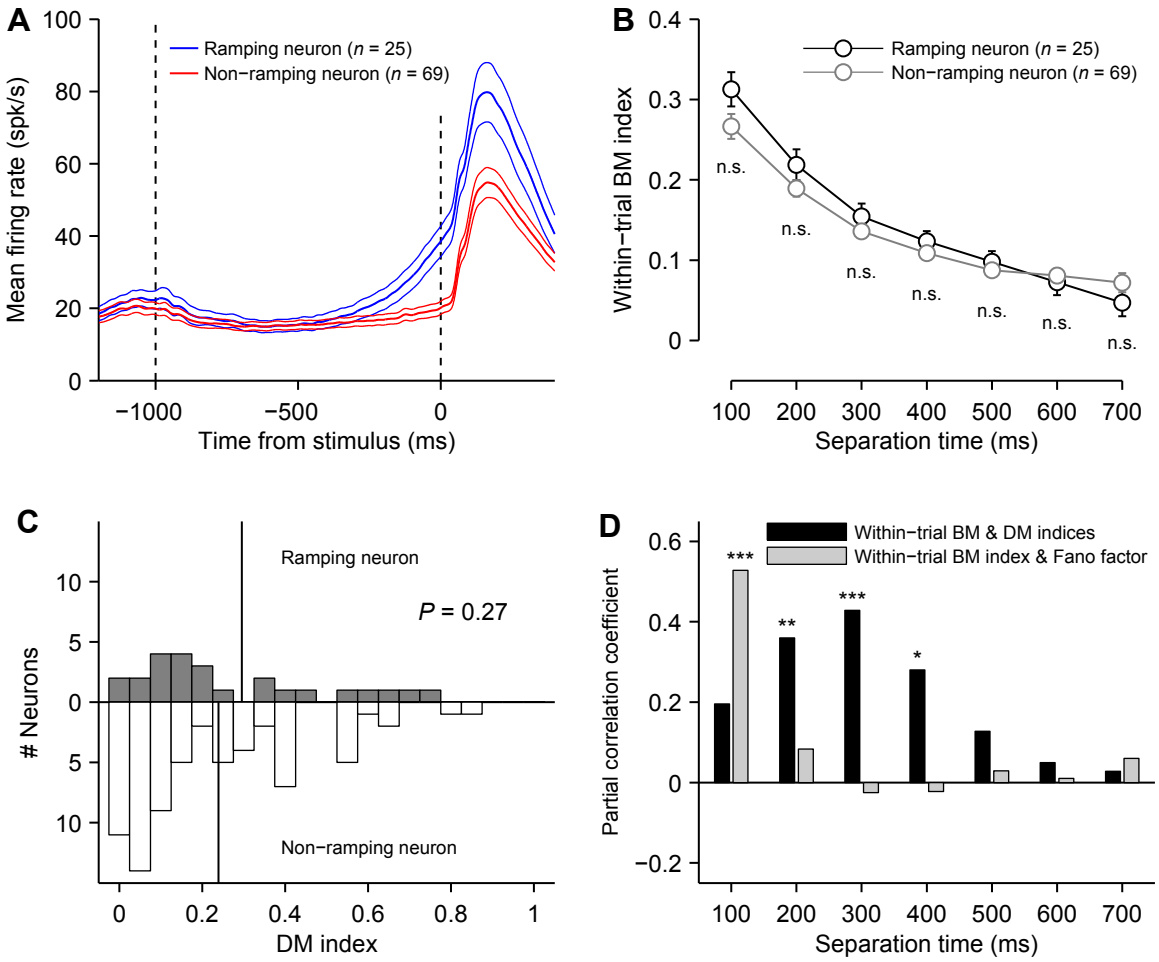

Supplementary Figure 7. The impact of ramp-like anticipatory responses in a pre-stimulus period. To specify neurons with baseline-activity modulation by anticipation, we focused on pre-stimulus activity occurring 200 ms prior to stimulus onset. If the pre-stimulus activity of a neuron differed significantly from the activity of the neuron 400–800 ms before stimulus onset (Mann-Whitney *U*-test, $P < 0.01$), and if the mean spike counts calculated from the 20 successive 10-ms time bins during that 200-ms period monotonically changed (Spearman's correlation, $\rho > 0.85$ or $\rho < -0.85$), the neuron was classified as a ramping neuron. If not, it was considered a non-ramping neuron. Of 94 LIP neurons, we found 25 ramping neurons and 69 non-ramping neurons. All of the 25 ramping neurons exhibited build-up changes in pre-stimulus activity (i.e. $\rho > 0.85$). (*A*) Average spike-density functions (mean ± *SE*) during the reaction-time task separately calculated from the subpopulations of the ramping (blue) and non-ramping neurons (red). Left and right vertical dashed lines indicate fixation onset and stimulus onset, respectively. (*B*) Average within-trial BM indices from ramping neurons (black; $n = 25$) and non-ramping neurons (gray; $n = 69$) as a function of separation time. No difference was found at all separation times (two-sample *t*-test, $P > 0.12$). (*C*) The distributions of DM indices from ramping (gray bar) and non-ramping neurons (white bar). The mean DM indices were not significantly different between the two groups (two-sample *t*-test, $P = 0.27$). (*D*) Partial correlation analysis using the indices obtained from only the non-ramping neurons. Conventions are the same as those used in Supplementary Figure 3*C*. The within-trial BM indices were significantly correlated with the DM indices and the Fano factors at separation times of 200–400 ms and 100 ms, respectively (Pearson's correlation, $P < 0.05$).

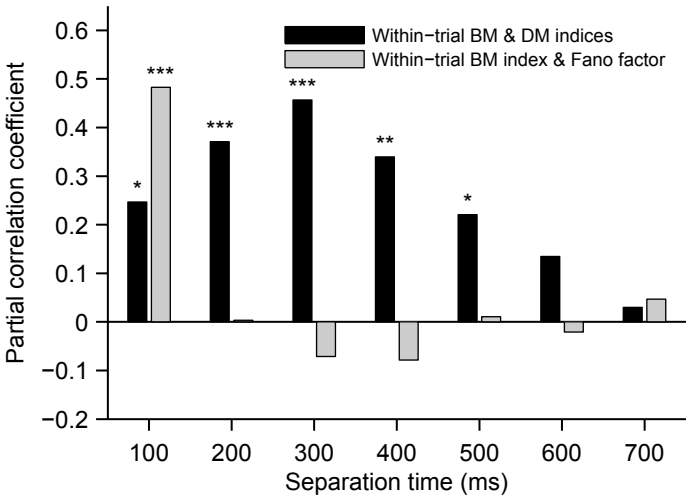

Supplementary Figure 8. Partial correlation analysis performed excluding fixation-related neurons. A neuron was defined as having fixation-related activity when its mean firing rate during an 800-ms period before stimulus onset was >2 *SD* above that 300 ms after the end of the inter-trial interval (Suzuki and Azuma 1977; Izawa et al. 2009). A total of 7 of 94 LIP neurons showed fixation-related activity. Significant partial correlations were preserved even using the dataset obtained from only neurons with no fixation-related activity (n = 87; Pearson's partial correlation, $P < 0.05$). Same conventions as in Supplementary Figure 3*C*.

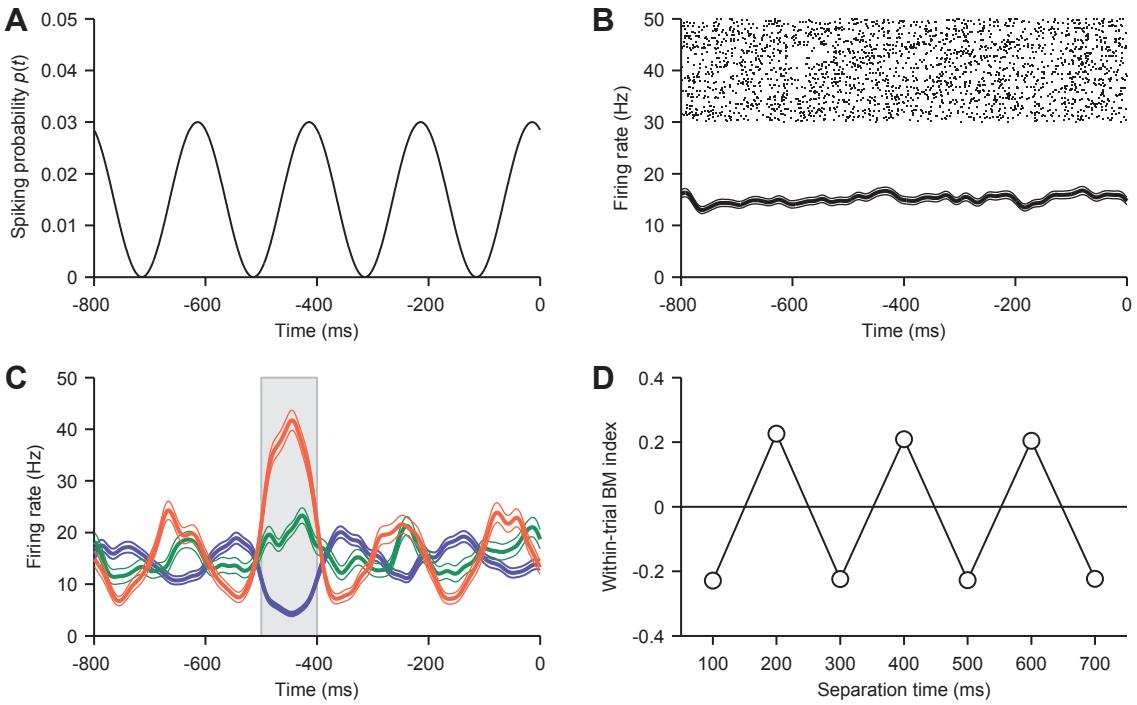

Supplementary Figure 9. Oscillatory activity and the within-trial BM index. The spiking probability as a function of time t (ms) was defined as $p(t) = A \cdot \sin(2\pi t/\theta + \varphi) + B$, where an amplitude A was 0.02 (spikes/ms), a cycle θ was 200 (ms), a phase φ was randomly selected from $-\pi$ (rad) to π (rad) in each trial, and B is constant (0.02 spikes/ms) indicating mean activity across trials. A spike train for each trial was constructed by randomly changing the phase of the neural oscillation from trial to trial. We computed spike-train datasets from 1,000 trials. (*A*) An example spiking probability for one trial. (*B*) Spike rasters in the first 200 trials (top) and the mean (±SE) spike-density function across 1,000 trials (bottom). (*C*) The spike-density functions of the high- (red), medium- (green), and low-activity (blue) groups which were classified according to the spike count during a 100-ms interval (gray rectangle). (*D*) Simulated within-trial BM indices as a function of separation time (bin size = 100 ms). The within-trial BM index had not only large positive values but also large negative values depending on separation time. Similar results were observed when a cycle θ was changed in the range from 150 ms to 800 ms. For the cycle which was around 100 ms or shorter, the within-trial BM index was close to zero irrespective of separation time.

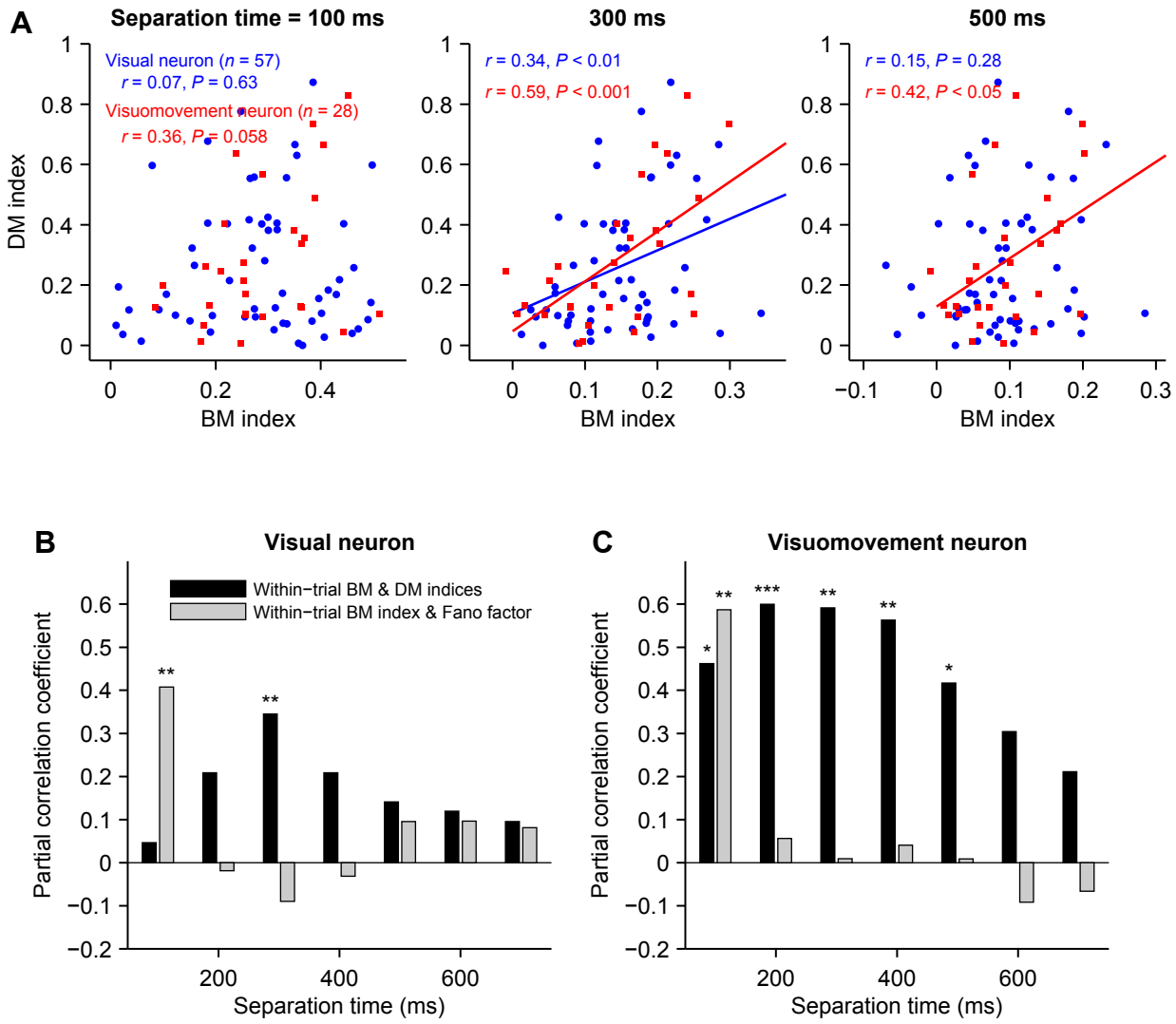

Supplementary Figure 10. Effects of neuron type on the correlation between baseline-activity maintenance, delay-period modulation, and trial-to-trial fluctuation. We classified LIP neurons into three neuron types: visual, movement, and visuomovement neurons (see Materials and Methods). (*A*) Relationship between DM and within-trial BM indices with respect to neuronal type. The BM indices were calculated with separation times of 100 ms (left), 300 ms (middle), and 500 ms (right). Blue circles and red rectangles indicate the data points obtained from the visual and visuomovement neurons, respectively. Lines indicate the least-squares fit to the data when the correlations were significant within each neuronal type (Pearson's correlation, $P < 0.05$). (*B*,*C*) Partial correlation analysis performed separately for visual (*B*) and visuomovement neurons (*C*). Conventions are the same as those used in Figure 6*D*. Movement neurons were excluded from these analyses, because of a small sample size ($n = 2$).

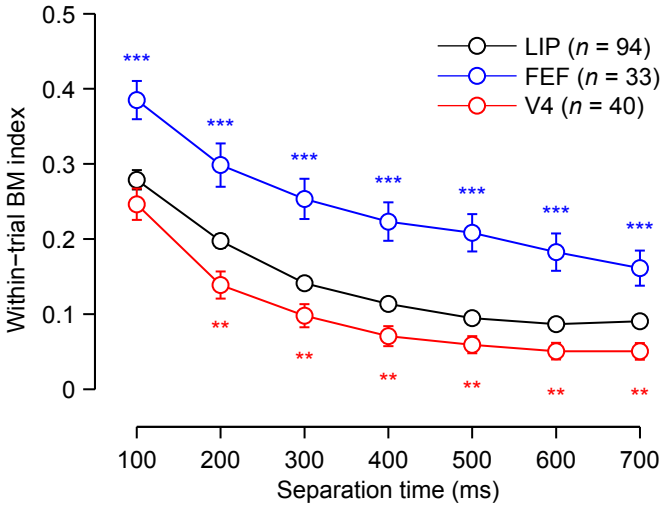

Supplementary Figure 11. Comparison of within-trial BM indices of LIP, FEF, and V4 neurons. Data sets for FEF and V4 neurons are from Ogawa and Komatsu (2010). The absolute values of Pearson's correlation coefficients were used as the BM index to match the analytical method to that used in the previous study. The mean within-trial BM indices for LIP neurons (black; n = 94) were significantly lower than those for FEF neurons (blue; n = 33) at all separation times, whereas they were significantly larger than those for V4 neurons (red; n = 40) at all separation times except 100 ms (two-sample t-test, ***P < 0.001, **P < 0.01). Error bars represent SE.

Supplementary Table 1. Correlation between the within-trial BM index and various variables. The coefficients (*r*) and *P* values of Pearson's correlations/partial correlations are summarized. Values shown in bold font indicate significant Pearson's r value at $P < 0.05$.

		Separation time (ms)						
		100	200	300	400	500	600	700
Correlation								
DM index	*r*	0.18	**0.37**	**0.44**	**0.33**	**0.22**	0.17	0.11
	P	0.08	**<0.001**	**<0.0001**	**<0.01**	**<0.05**	0.1	0.28
Fano factor (FF)	*r*	**0.47**	0.05	-0.03	-0.04	0.03	-0.00002	0.05
	P	**<0.0001**	0.65	0.78	0.72	0.74	0.99	0.65
Performance score	*r*	0.06	0.15	0.14	0.11	-0.03	-0.03	0.01
	P	0.56	0.14	0.19	0.29	0.78	0.8	0.89
Saccadic reaction time	*r*	-0.09	-0.13	-0.1	-0.09	-0.07	-0.07	0.03
	P	0.39	0.21	0.36	0.39	0.51	0.53	0.76
Microsaccade rate	*r*	-0.11	-0.1	-0.07	-0.13	-0.05	0.003	0.08
	P	0.29	0.32	0.52	0.22	0.6	0.98	0.43
Partial correlation								
DM index factoring out FF	*r*	0.19	**0.37**	**0.44**	**0.34**	**0.22**	0.17	0.11
	P	0.08	**<0.001**	**<0.0001**	**<0.01**	**<0.05**	0.1	0.29
FF factoring out DM index	*r*	**0.47**	0.04	-0.05	-0.05	0.03	-0.01	0.04
	P	**<0.0001**	0.73	0.64	0.62	0.8	0.95	0.67